On the properties of the Alfvén transition zone separating the solar corona and the solar wind

Rohit Chhiber

NASA Goddard Space Flight Center & University of Delaware

Collaborators: Francesco Pecora, Arcadi Usmanov, William Matthaeus, Steven Cranmer, Melvyn Goldstein

Annual International Astrophysics Conference

[Bracketing the Solar Wind: The Physics of its Initiation and Termination]

26th Mar 2024, Turin, Italy

Solar corona vs solar wind – where is the boundary?

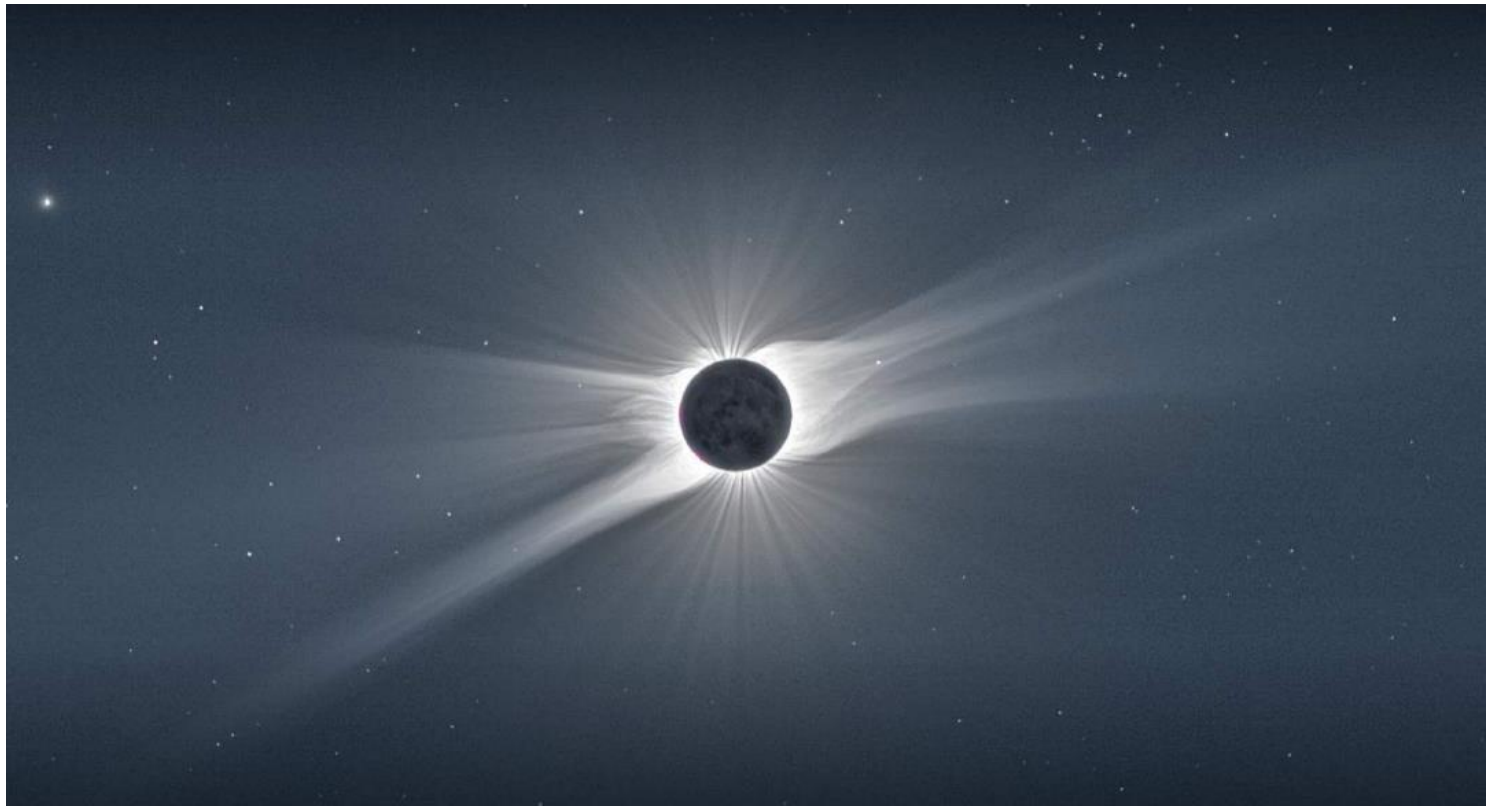

Image credit: Dr. Steve Cranmer

Critical points/surfaces -

- Flow becomes supersonic at the sonic surface
- Super-Alfvenic at Alfven surface
- $\beta = 1$ surface; magnetosonic surface

Outline

- Introduction and overview of Alfvén surface
- Turbulence; Extended and fragmented Alfvén zone in global model
- Global properties of Alfvén zone from Parker Solar Probe observations and model
- Stochastic propagation of Alfvén waves in the Alfvén zone
- Conclusions

The Alfven "radius"

r_A is distance where $U > V_A$, where $V_A = \frac{B}{\sqrt{4\pi\rho}}$

- Below r_A, information (waves) can propagate both Sunward & outward.
  Above r_A, the solar wind drags out both inward & outward modes
- Strong transfer of angular momentum from Sun to wind below r_A; Below r_A, magnetic field maintains ~rigid rotation with Sun (Weber & Davis 1967)
- Some models of magnetic field "switchback" formation invoke K-H instability above r_A (Ruffolo+ 2020)

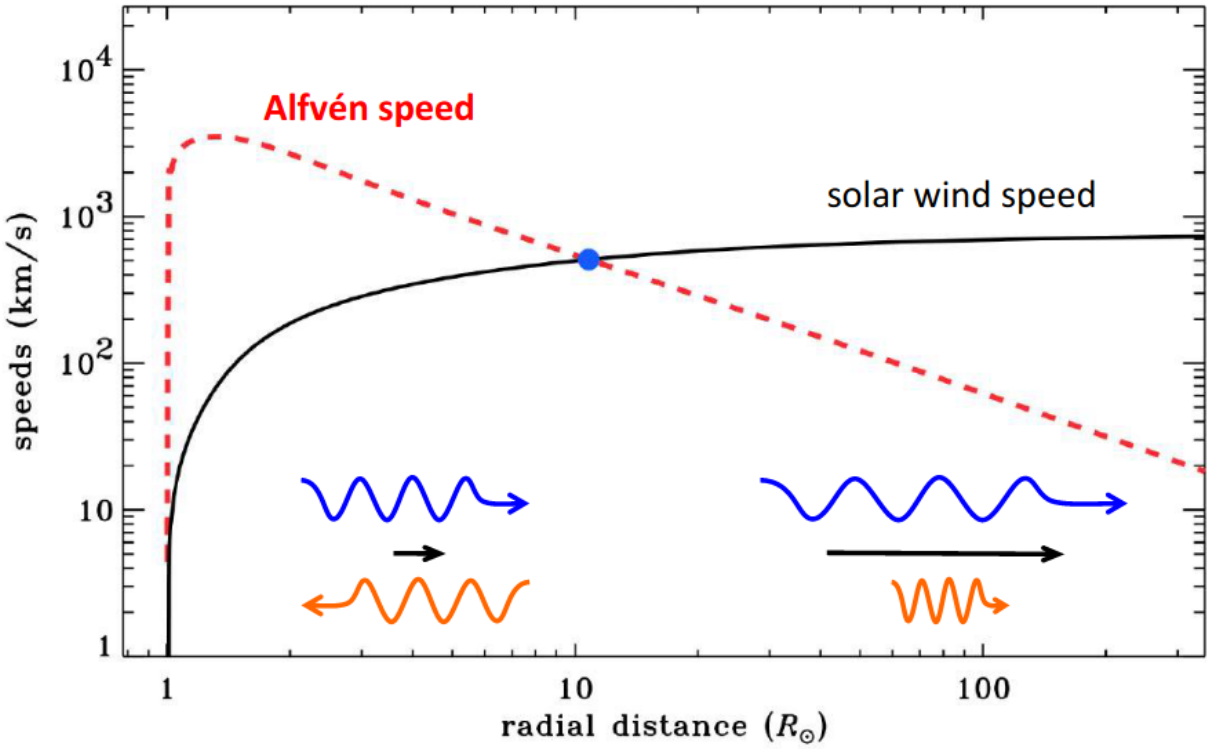

Credit: Dr. Steve Cranmer

Alfven surface in 3D MHD simulations of global solar wind

Large-scale variability – solar-source related; solar activity effects

Solar min

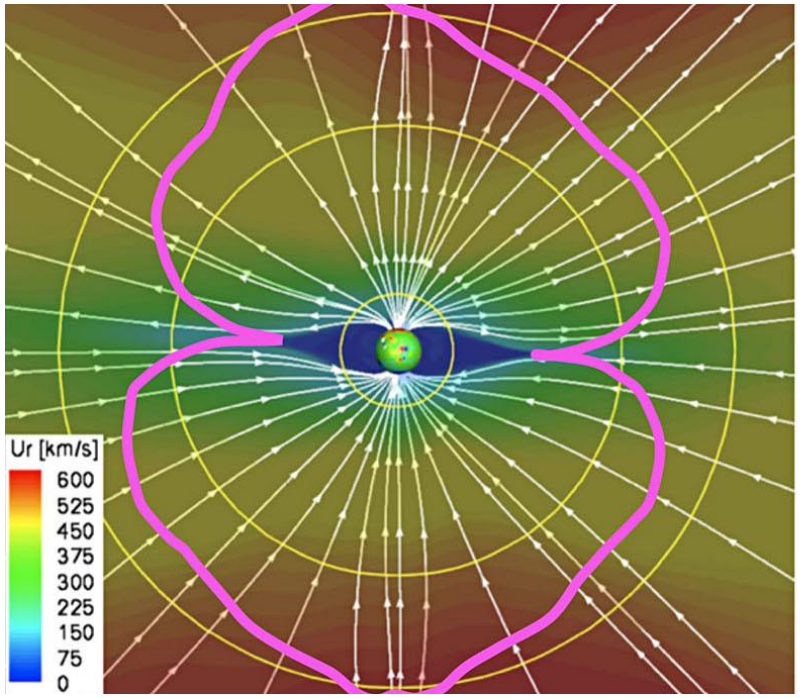

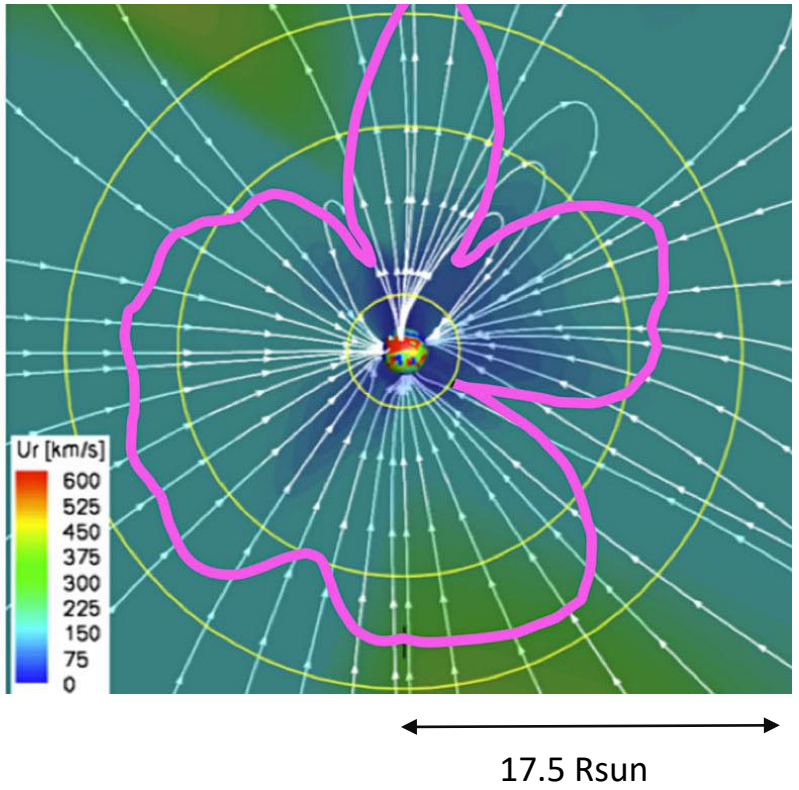

Solar max

Meridional planes (Cohen 2015; PUNCH website)

Hints of a corrugated/fragmented Alfven surface/zone

DeForest+ 2018; *STEREO*

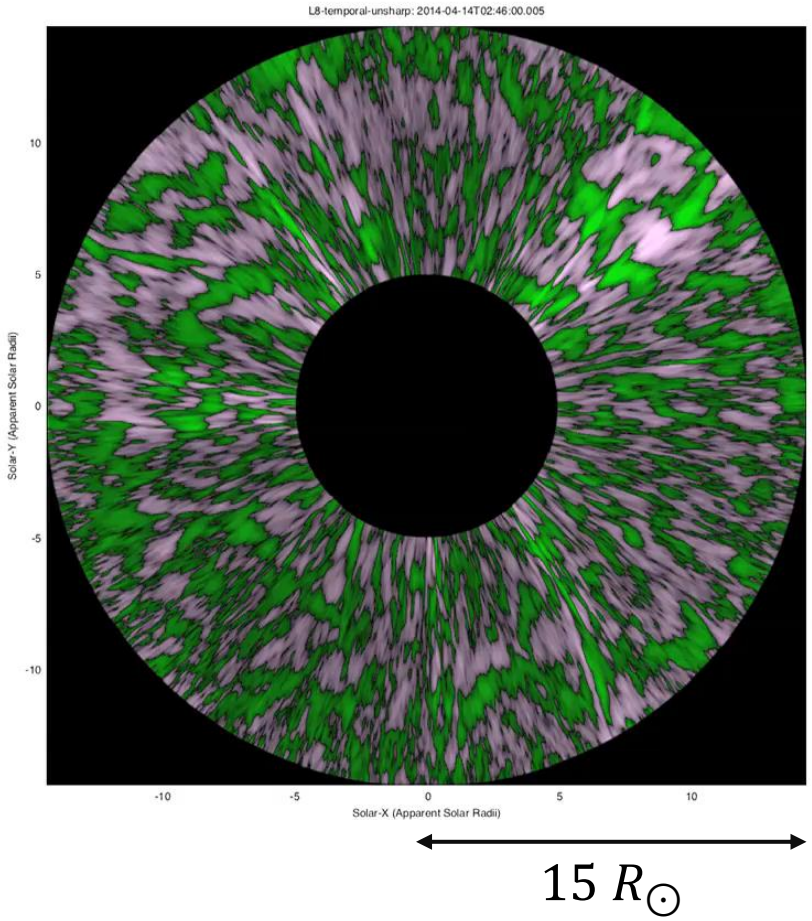

$15\ R_\odot$

Lotova+ (1985, 1997); radio scintillation

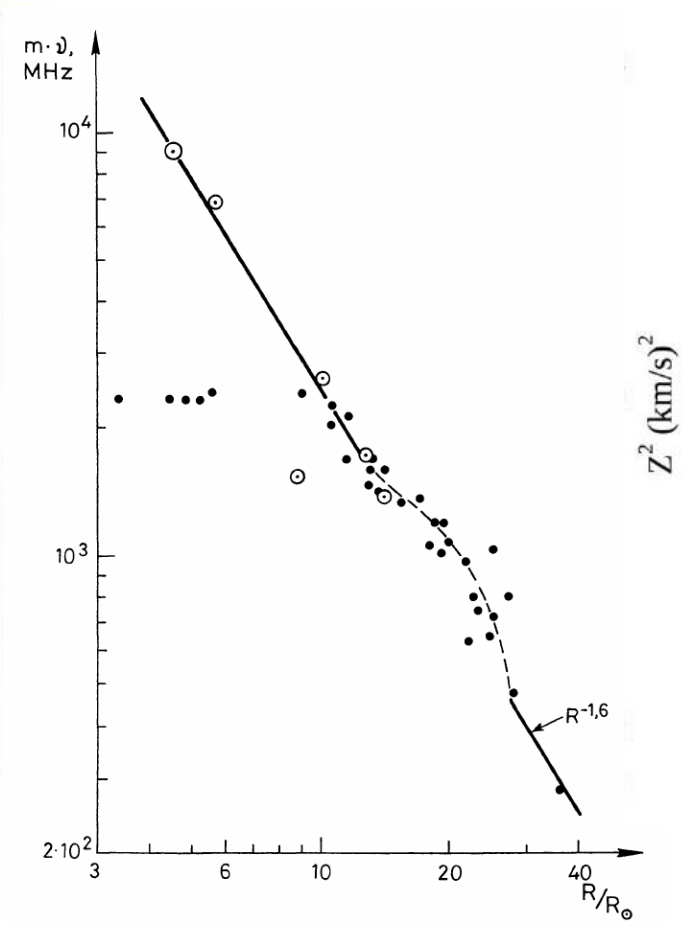

Chhiber+ 2019; SW sim w' turbulence transport

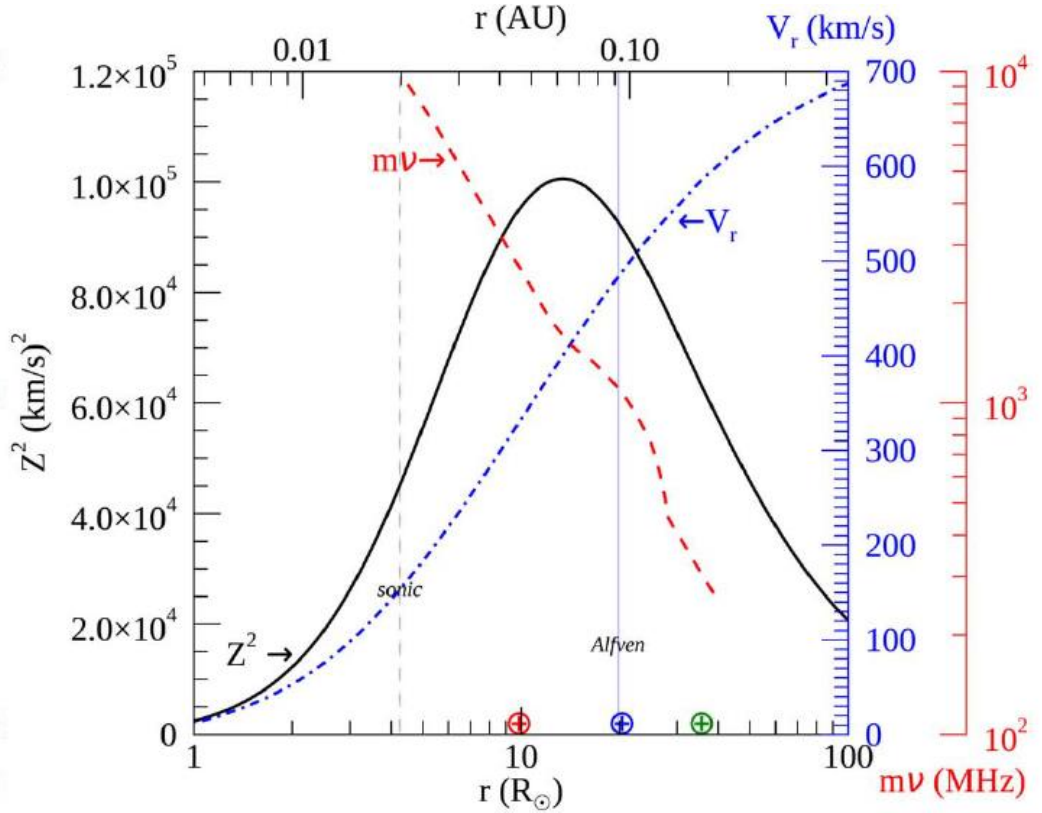

- ρ, V, B fluctuations imply fluctuations in M_A

$$M_{\mathrm{A}}(\mathbf{r}) = \frac{V_{\mathrm{sw}}}{V_{\mathrm{A}}} = \frac{V_{\mathrm{sw}}(\mathbf{r})}{B(\mathbf{r})/\sqrt{4\pi\rho(\mathbf{r})}}$$

Corrugated Alfven surface - Recent in situ observations

Verscharen+ 2021; *Ulysses*

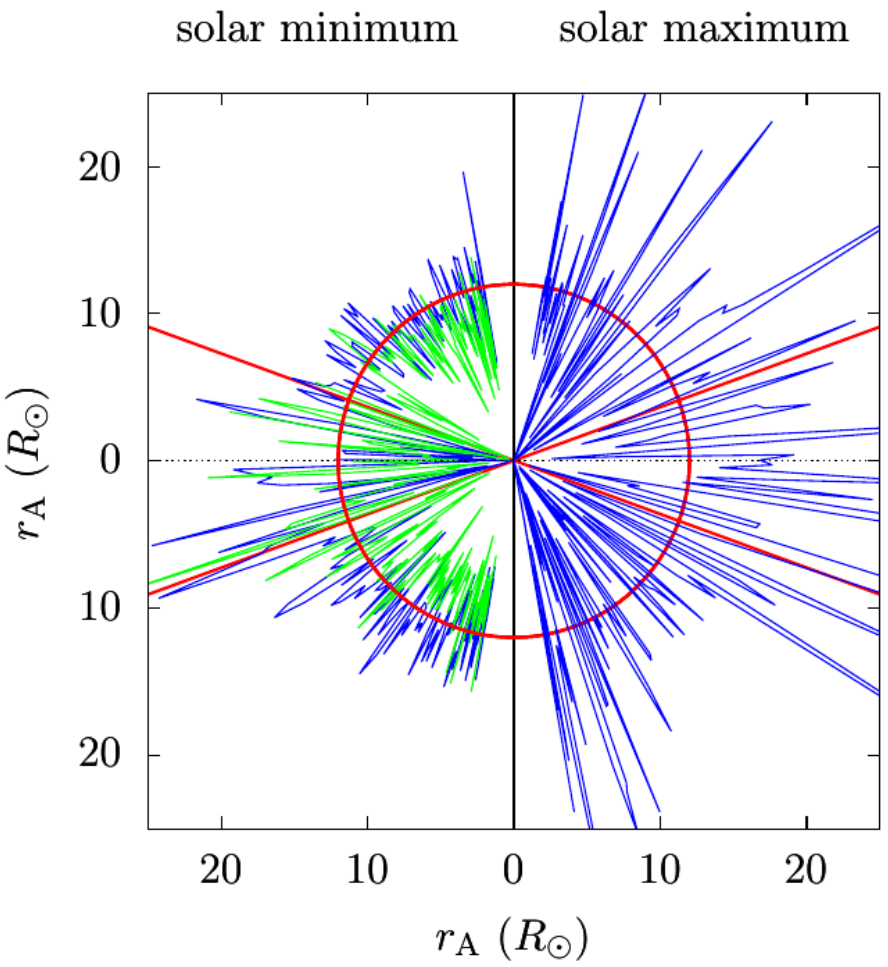

Variability in heliolatitude

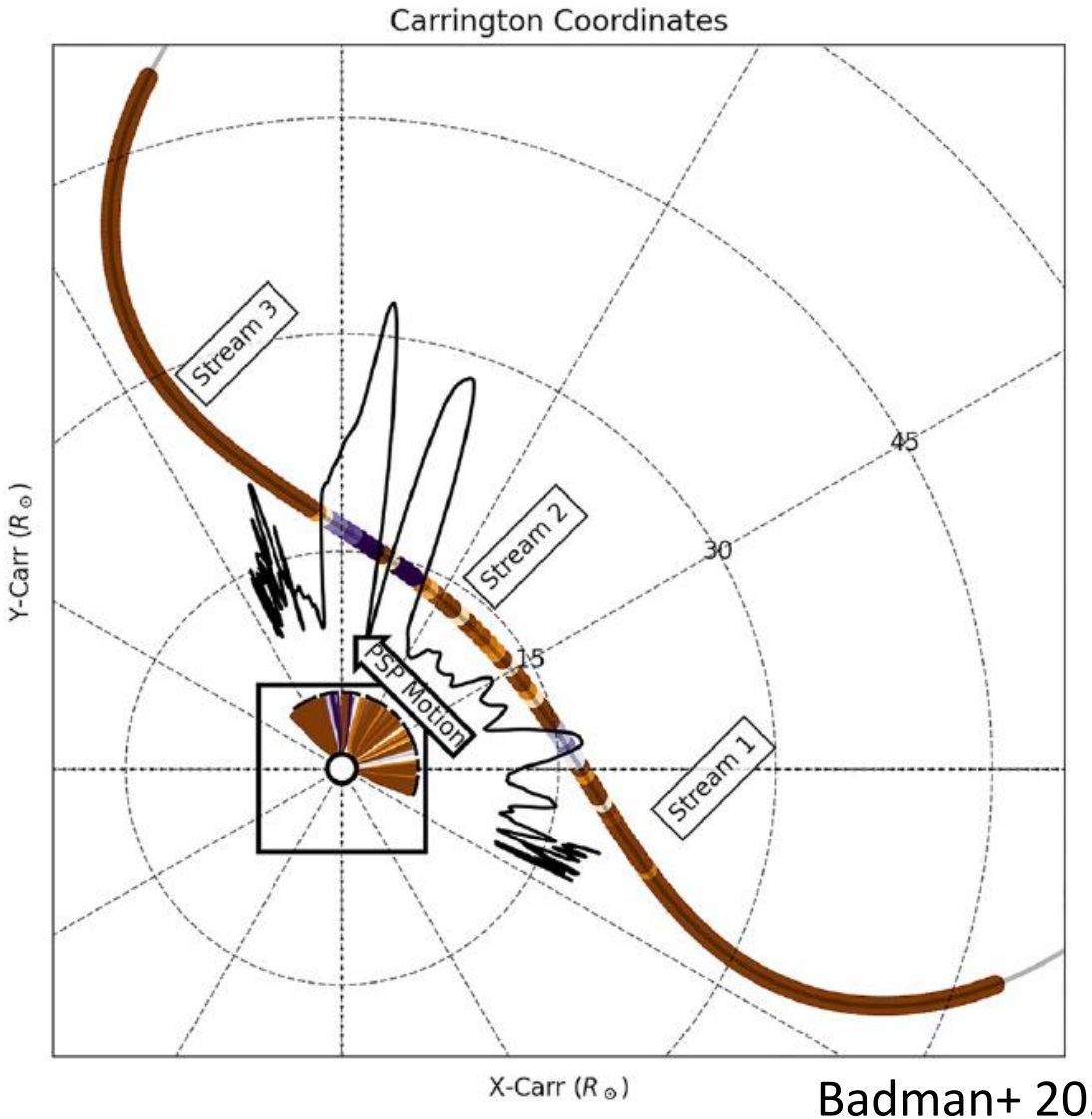

Badman+ 2023; *PSP*

Variability in heliolongitude

Outline

- Introduction and overview of Alfvén surface
- Turbulence; Extended and fragmented Alfvén zone in global model
- Global properties of Alfvén zone from Parker Solar Probe observations and model
- Stochastic propagation of Alfvén waves in the Alfvén zone
- Conclusions

Turbulence in the Solar Wind

- Solar wind is known to be turbulent, with structure and fluctuations across scales
- Turbulent cascade can provide a mechanism for coronal heating, and acceleration and heating of the solar wind
- Fluctuations can influence several physical processes in interplanetary space, including transport of SEPs

Belcher & Davis 1971

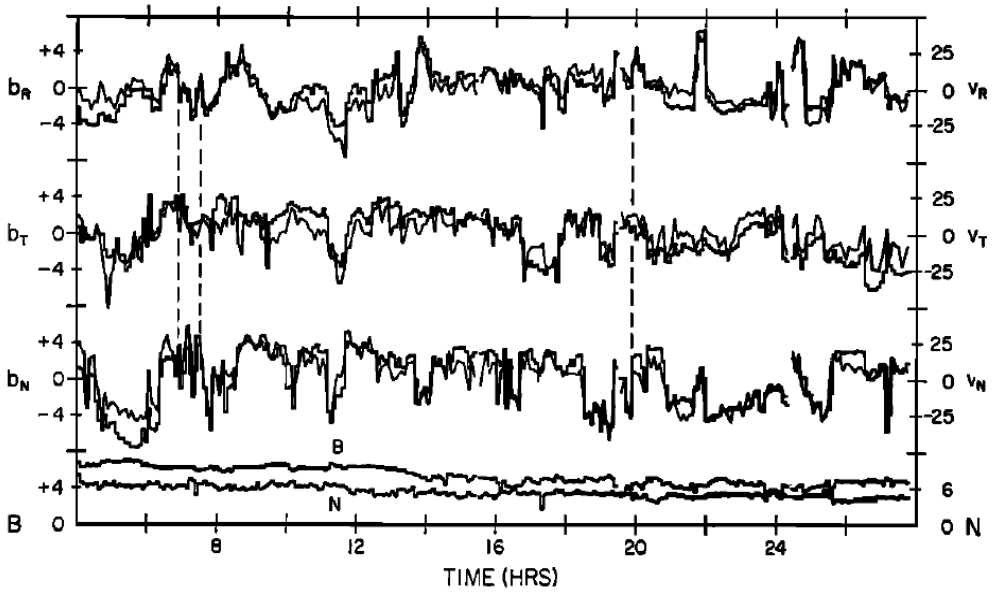

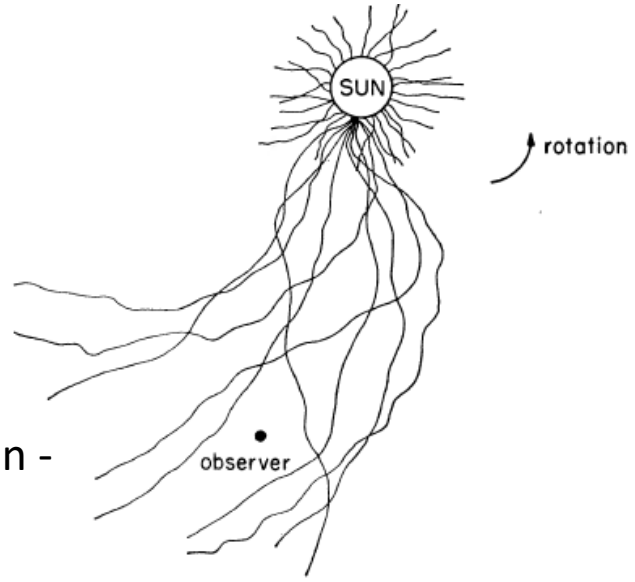

Fieldline diffusion - Jokipii & Parker 1969

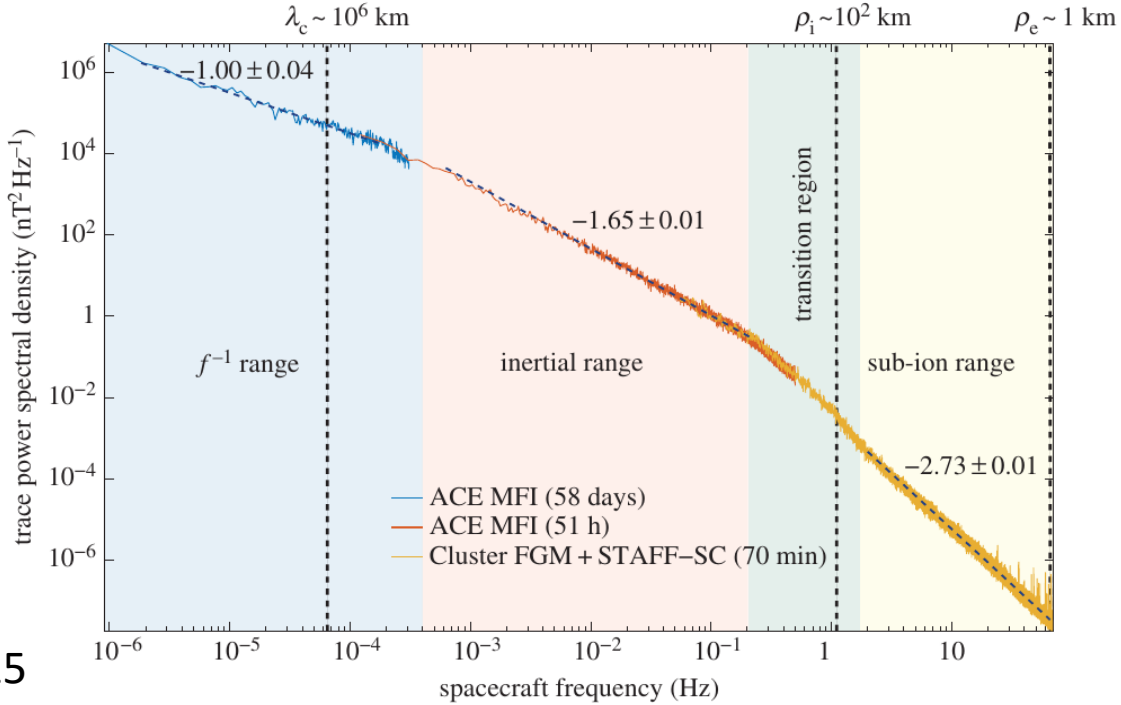

Kiyani+ 2015

Global simulation with turbulence modeling – Schematic of Reynolds-Averaging Approach

- Global simulation of corona/solar wind cannot explicitly resolve turbulence
- Reynolds decomposition splits fields (ã) into mean (a) and fluctuation (a'; arbitrary amplitude)

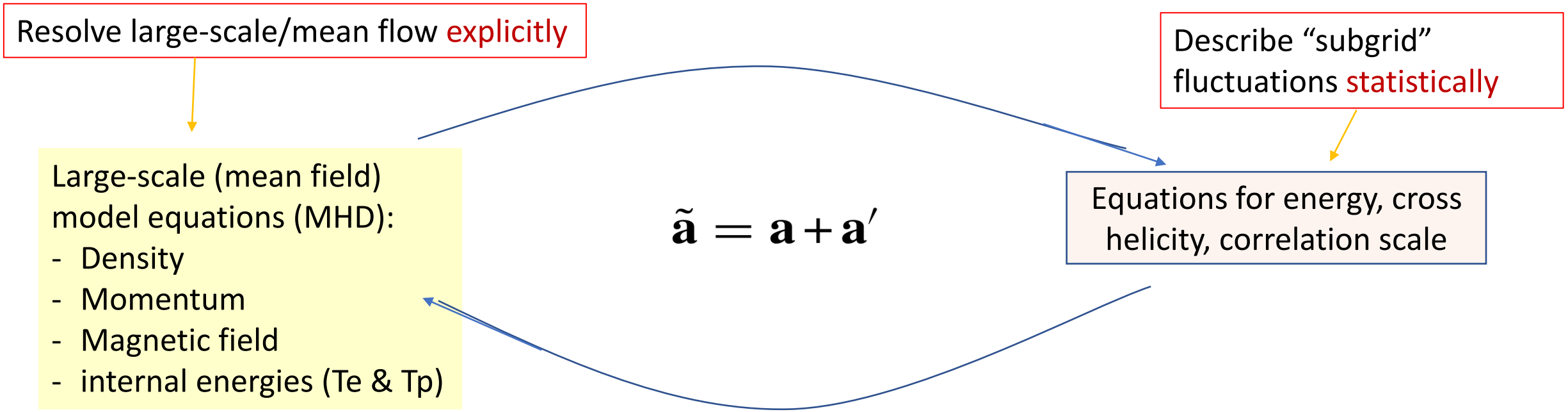

- Two-way coupling – turbulence accelerates and heats wind, and gradients in large-scale fields drive turbulence
- Well-tested, good agreement with observations (Usmanov+ 2018, Chhiber+ 2021)

Alfven Mach number and fragmented Alfven zone

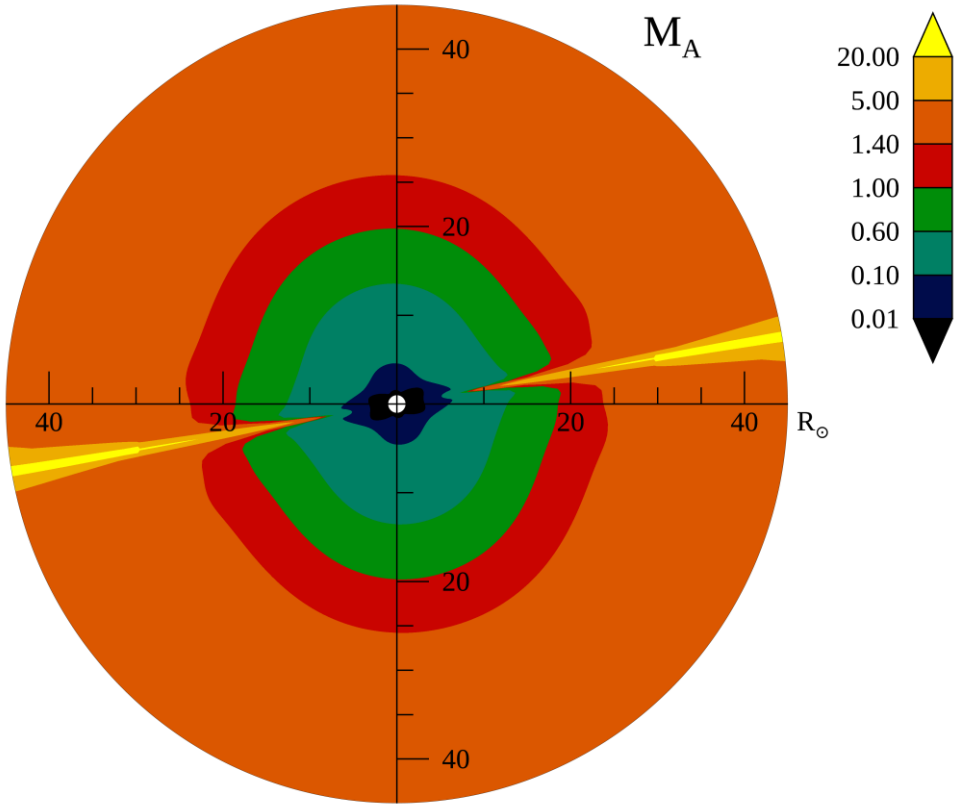

- Meridional plane
- Computed using mean fields

$$M_A(\mathbf{r}) = \frac{V_{sw}}{V_A} = \frac{V_{sw}(\mathbf{r})}{B(\mathbf{r})/\sqrt{4\pi\rho(\mathbf{r})}}$$

Alfven Mach number and fragmented Alfven zone

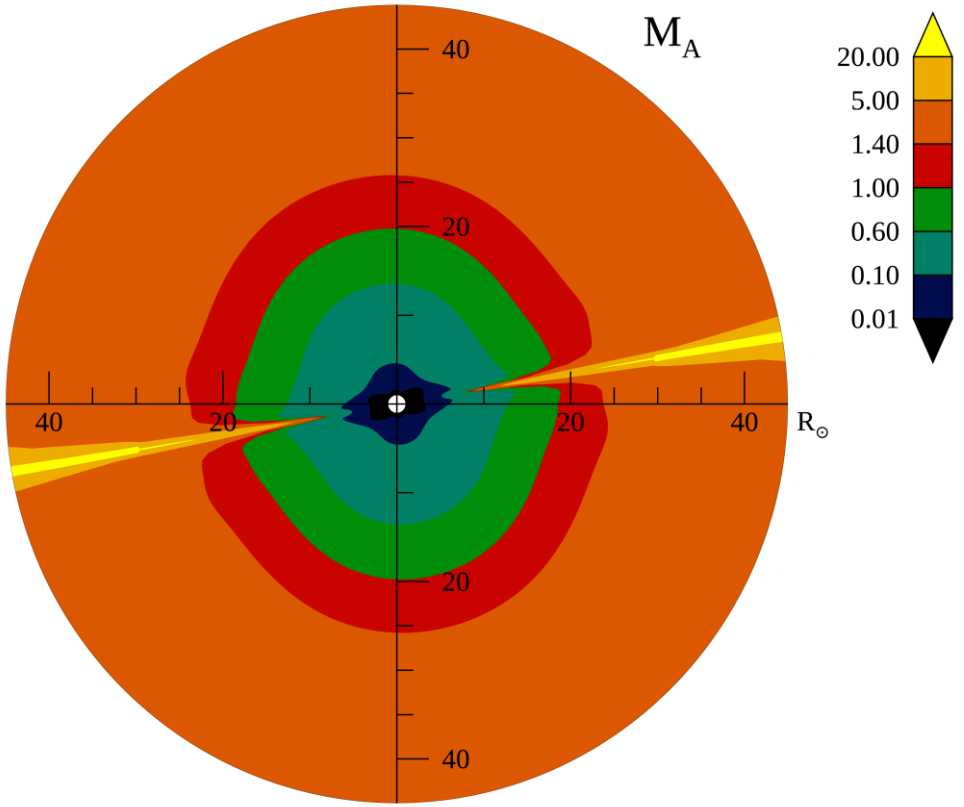

- Meridional plane
- Computed using mean fields

$$M_{\mathrm{A}}(\mathbf{r}) = \frac{V_{\mathrm{sw}}}{V_{\mathrm{A}}} = \frac{V_{\mathrm{sw}}(\mathbf{r})}{B(\mathbf{r})/\sqrt{4\pi\rho(\mathbf{r})}}$$

Explicit fluctuations (synthetic, but *constrained by turbulence model*) -

- $Z^2 \rightarrow \delta B_{rms} \rightarrow \delta B$
- At each simulation grid point a random magnetic fluctuation δB is generated, from a Gaussian distribution with standard dev. equal to δB_{rms} at that grid point
- $V_A = |\boldsymbol{B} + \delta \boldsymbol{B}|/\sqrt{4\pi\rho}$

Alfven Mach number and fragmented Alfven zone

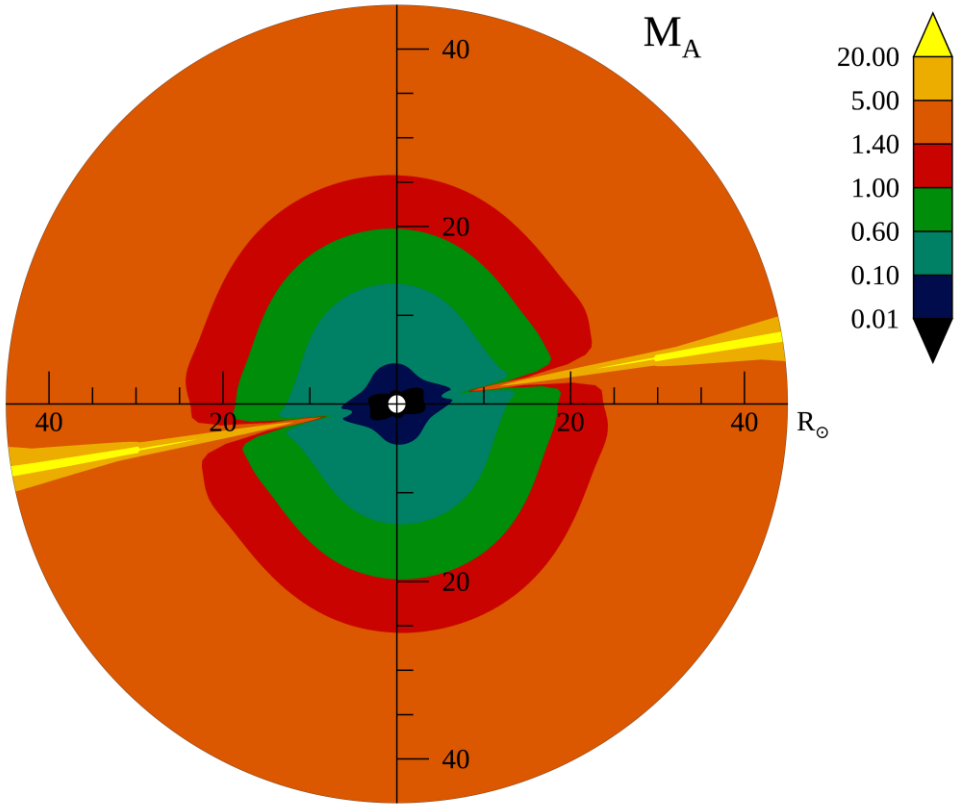

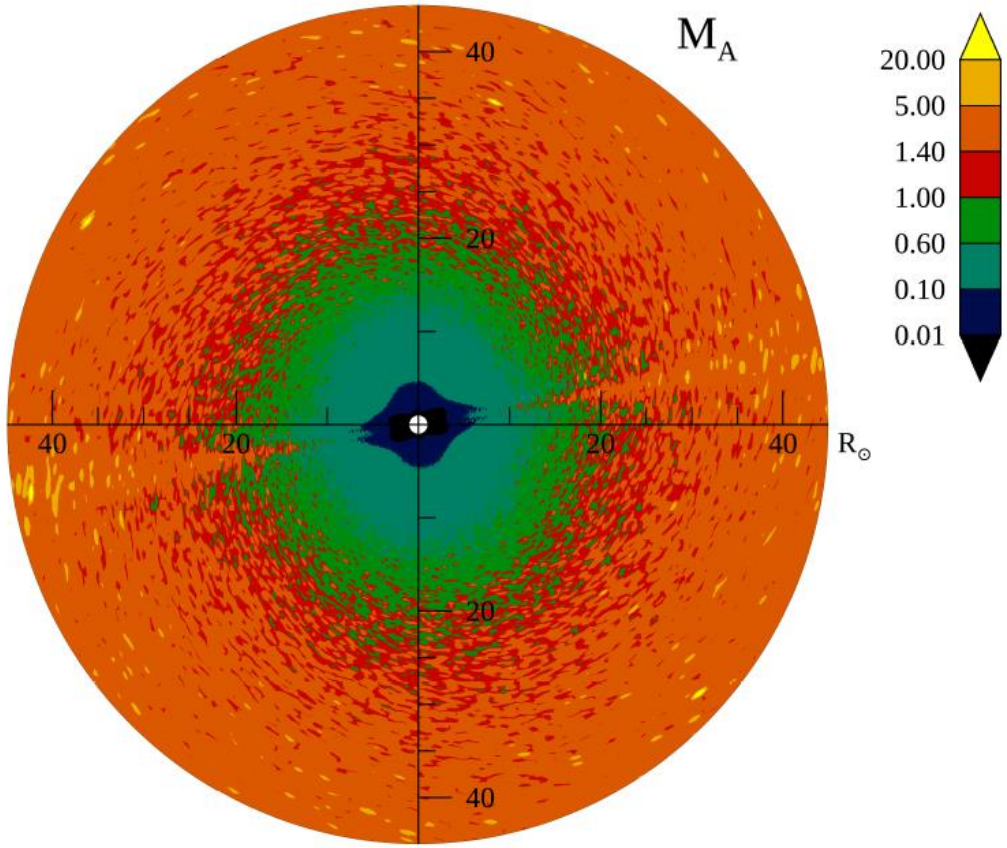

- Meridional plane
- Computed using mean fields

$$M_A(\mathbf{r}) = \frac{V_{sw}}{V_A} = \frac{V_{sw}(\mathbf{r})}{B(\mathbf{r})/\sqrt{4\pi\rho(\mathbf{r})}}$$

Explicit fluctuations (synthetic, but *constrained by turbulence model*) -

- $Z^2 \rightarrow \delta B_{rms} \rightarrow \delta B$
- At each simulation grid point a random magnetic fluctuation δB is generated, from a Gaussian distribution with standard dev. equal to δB_{rms} at that grid point
- $V_A = |\boldsymbol{B} + \delta \boldsymbol{B}|/\sqrt{4\pi\rho}$

Fragmented Alfven zone

Solar equatorial plane

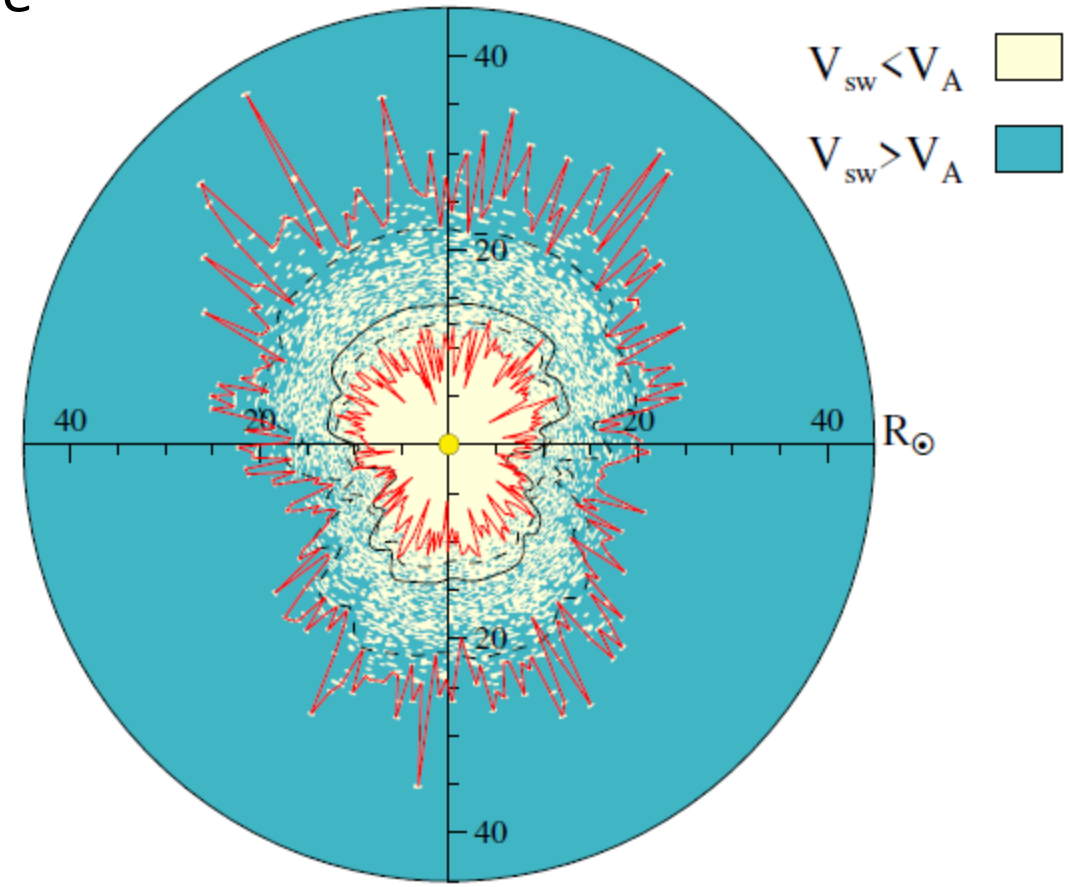

Meridional plane

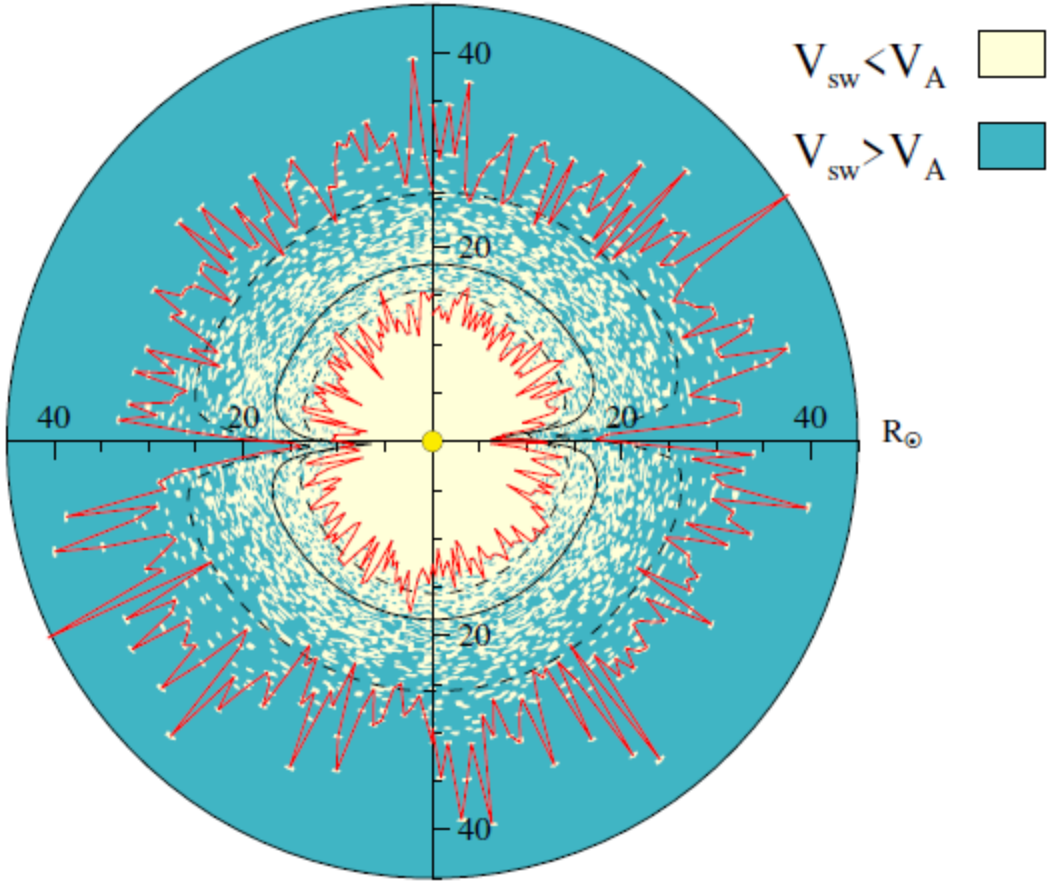

Chhiber et al. 2022, *MNRAS*

Comparison with PSP observations

Virtual PSP trajectory along sim driven by magnetograms corresponding to PSP E1 and E8

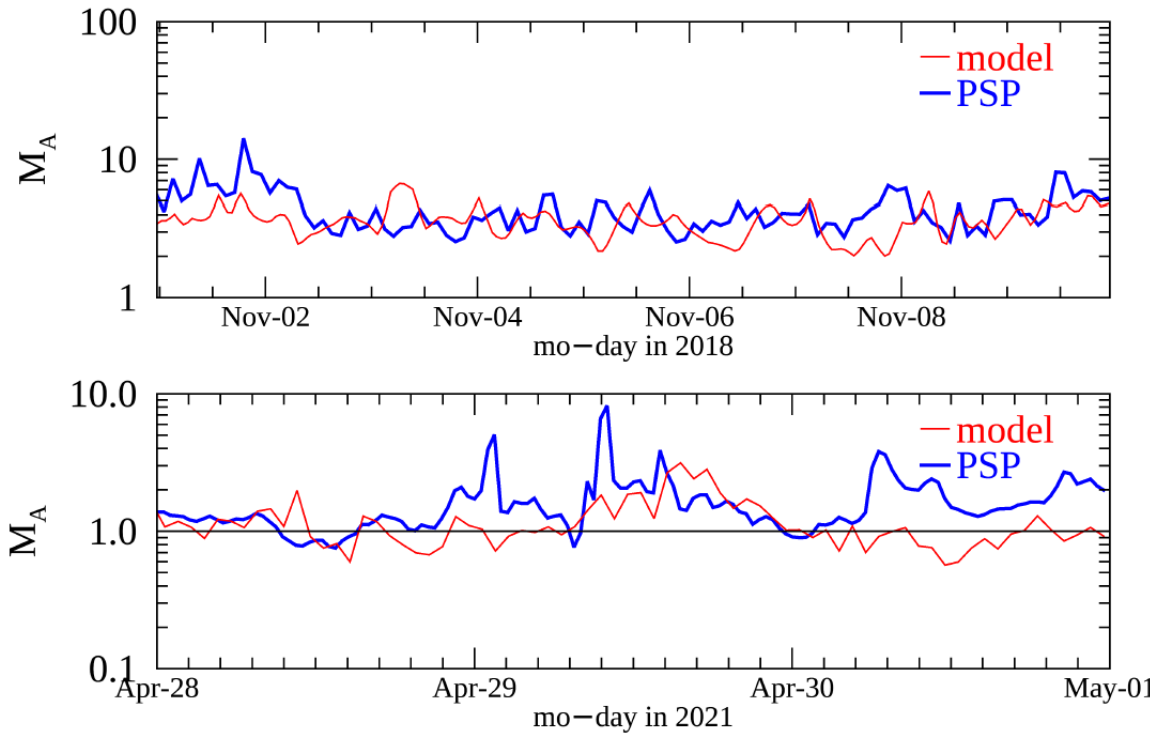

Probability of Alfvenic transition as a function of helioradius

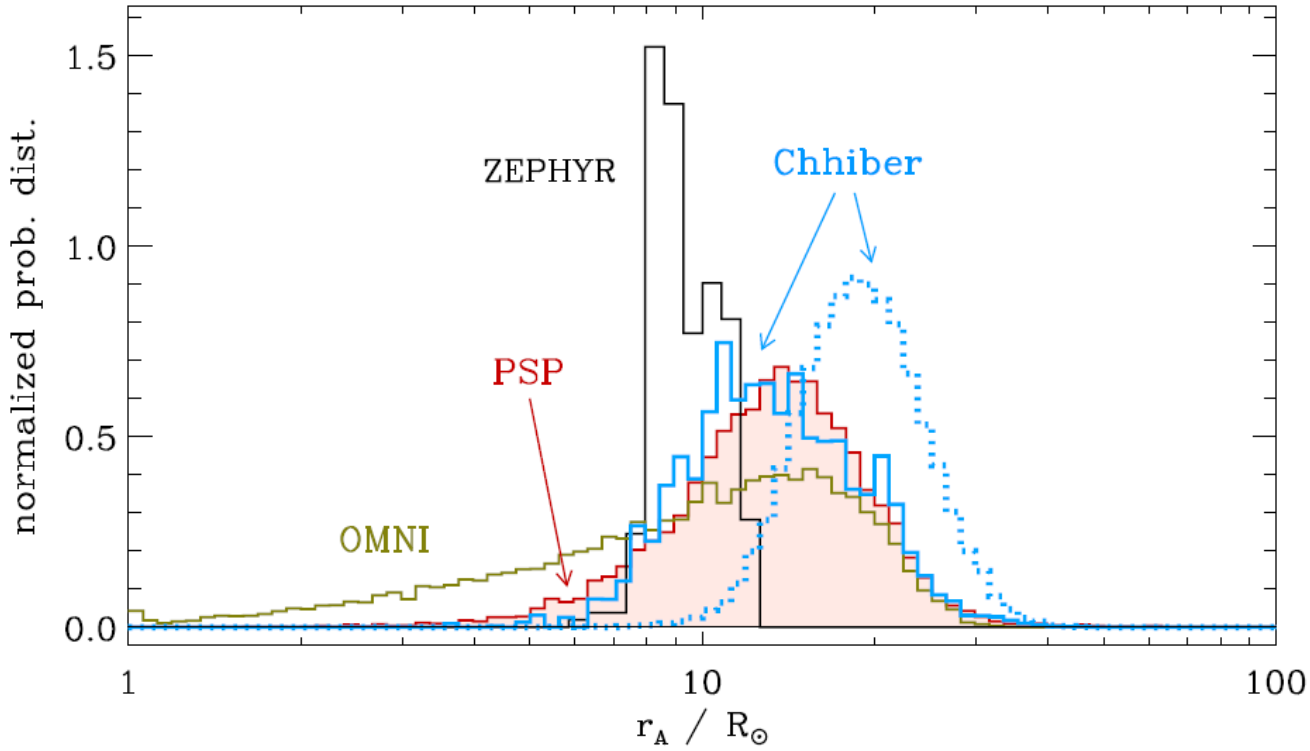

Chhiber+ 2022, *MNRAS*

Cranmer+ 2023, *Solar Phys.*

Outline

- Introduction and overview of Alfvén surface
- Turbulence; Extended and fragmented Alfvén zone in global model
- Global properties of Alfvén zone from Parker Solar Probe observations and model
- Stochastic propagation of Alfvén waves in the Alfvén zone
- Conclusions

Global properties of Alfven zone – PSP and Model

- PSP data E 8 – 14
- Data resampled to 1-min cadence
- Identified subAlfvenic periods longer than 10 min duration

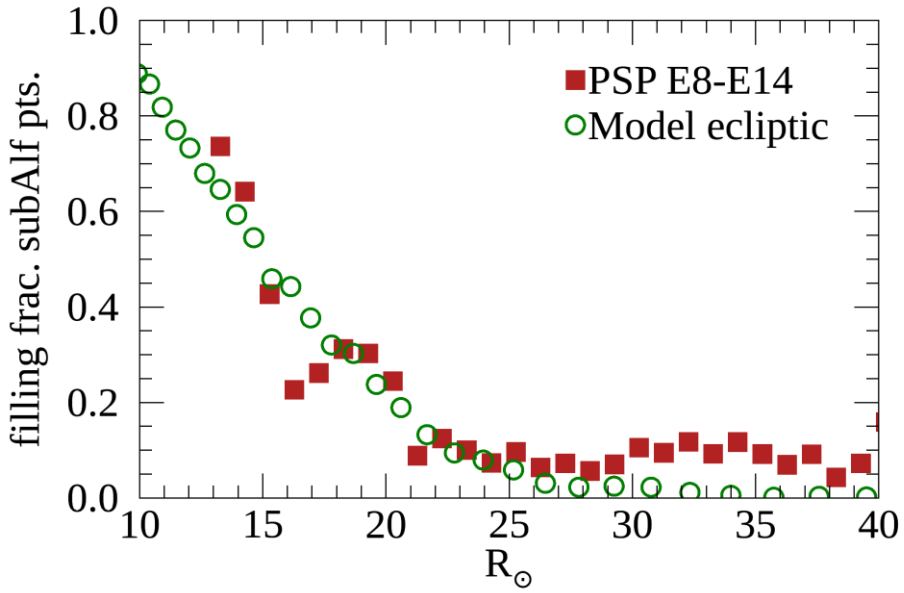

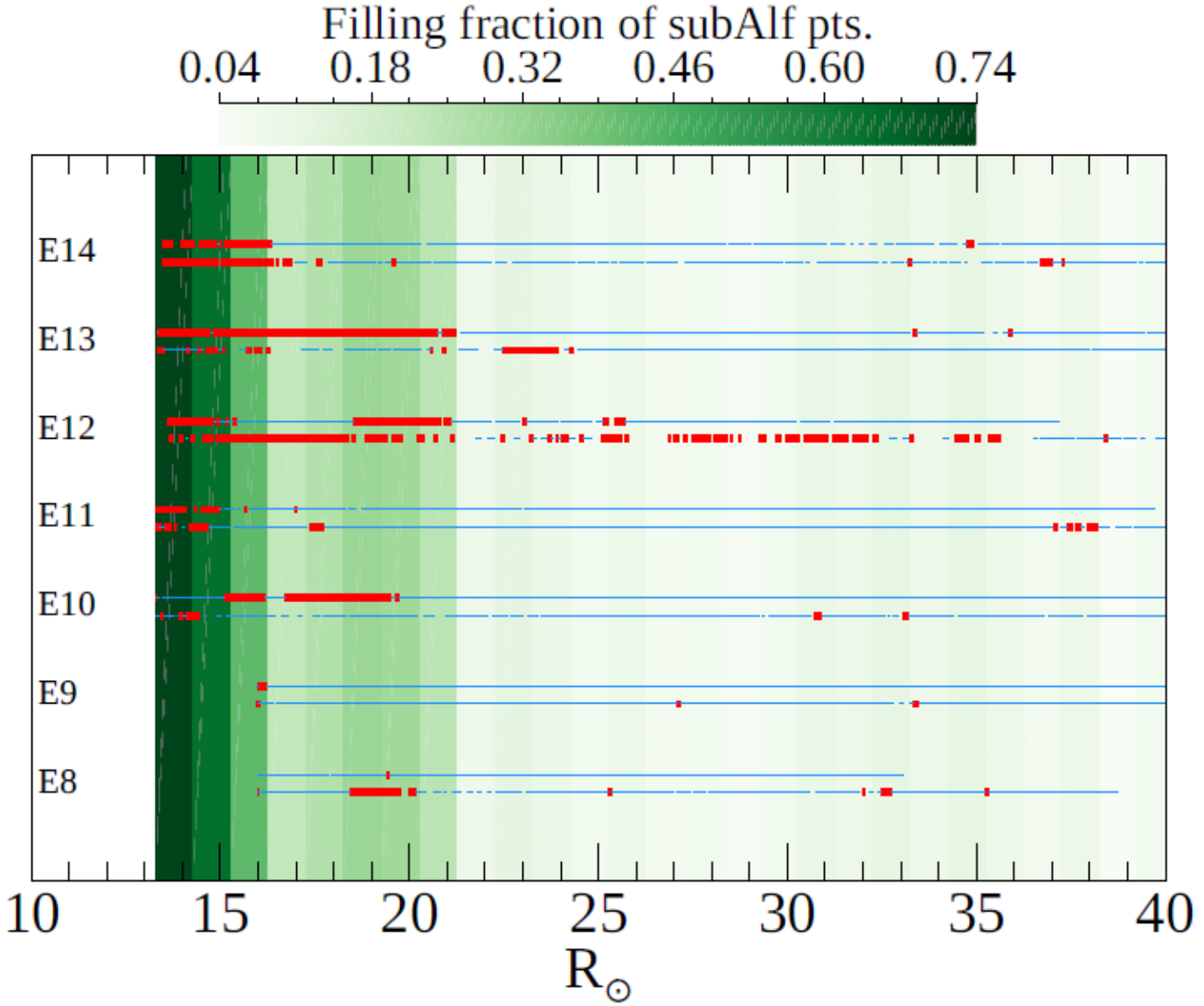

Chhiber+ 2024, *in prep*

Joint distributions of subAlfvenic-interval duration and heliodistance

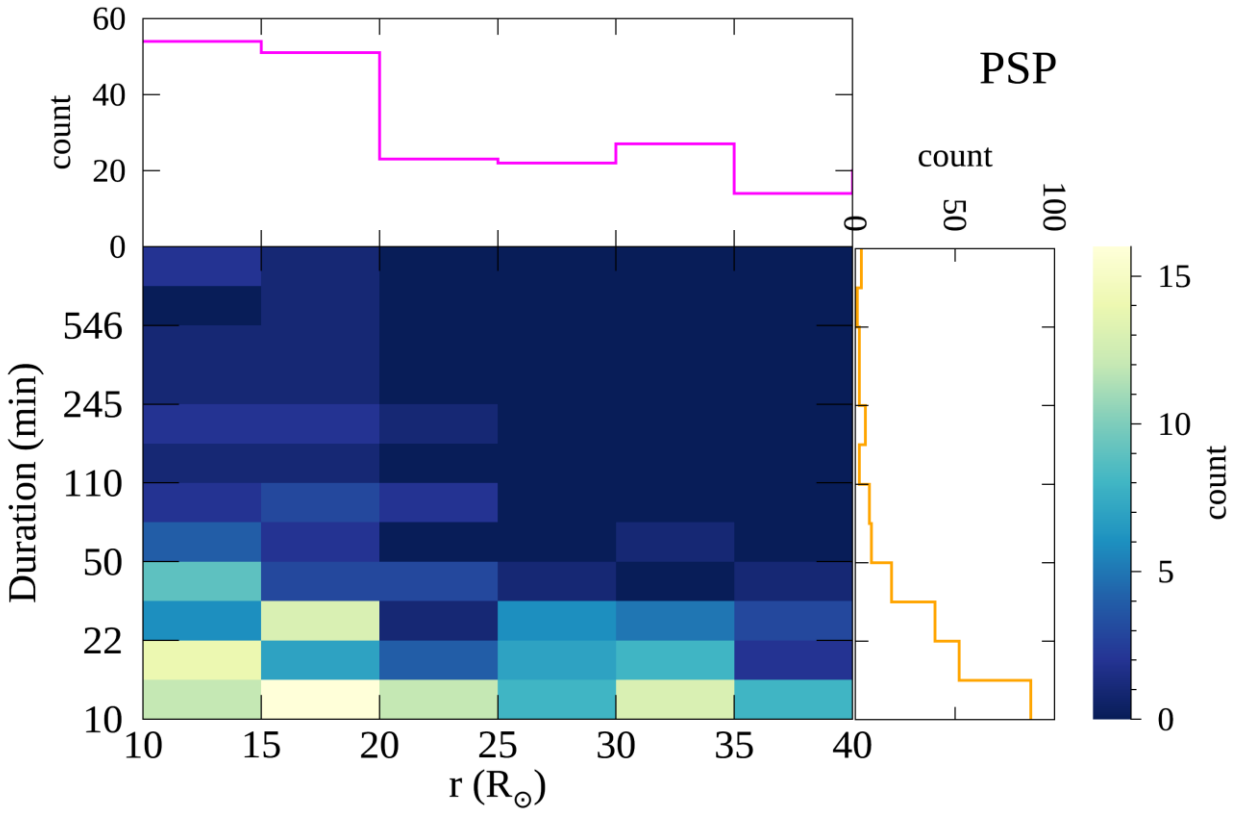

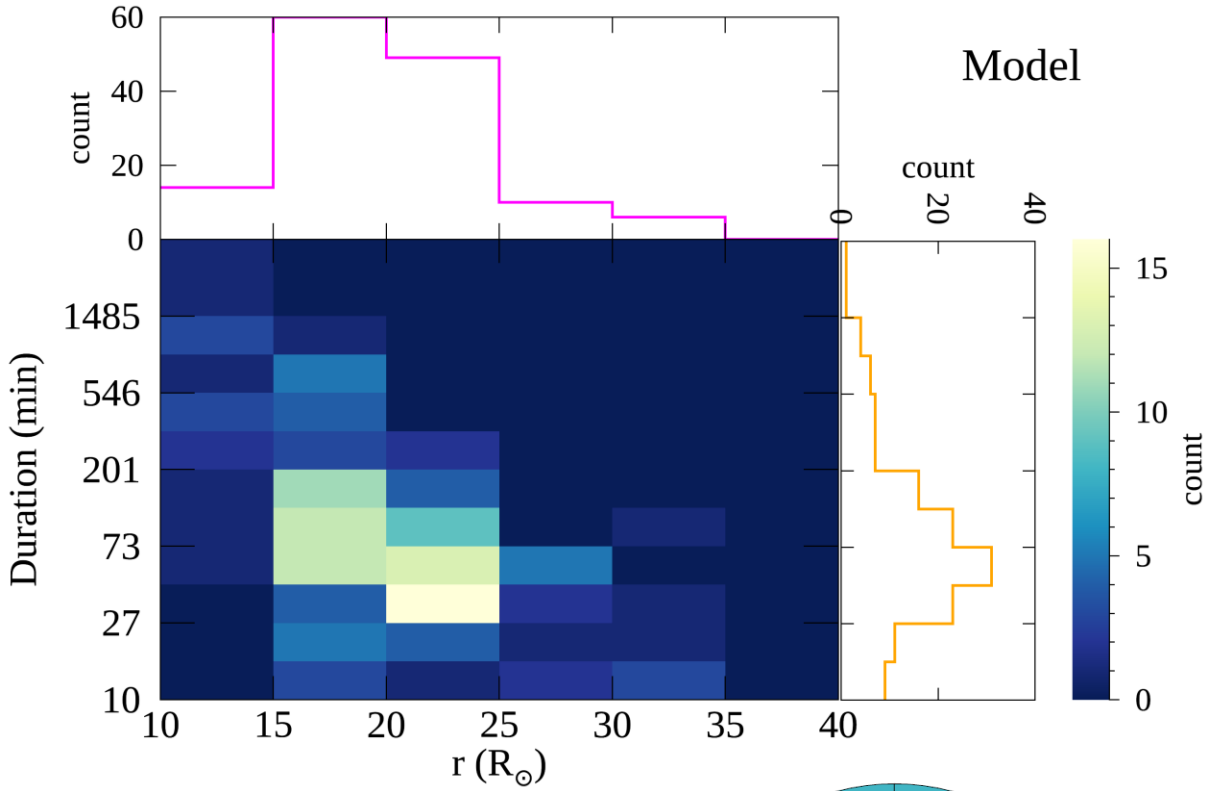

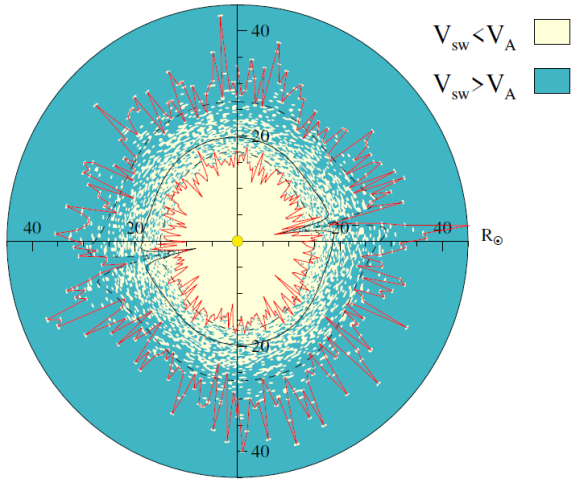

Chhiber+ 2022 prediction on Alfven zone – both frequency and duration/size of subAlfvenic intervals will increase approaching Sun

Chhiber+ 2024, *in prep*

Joint distributions of subAlfvenic interval duration and heliodistance

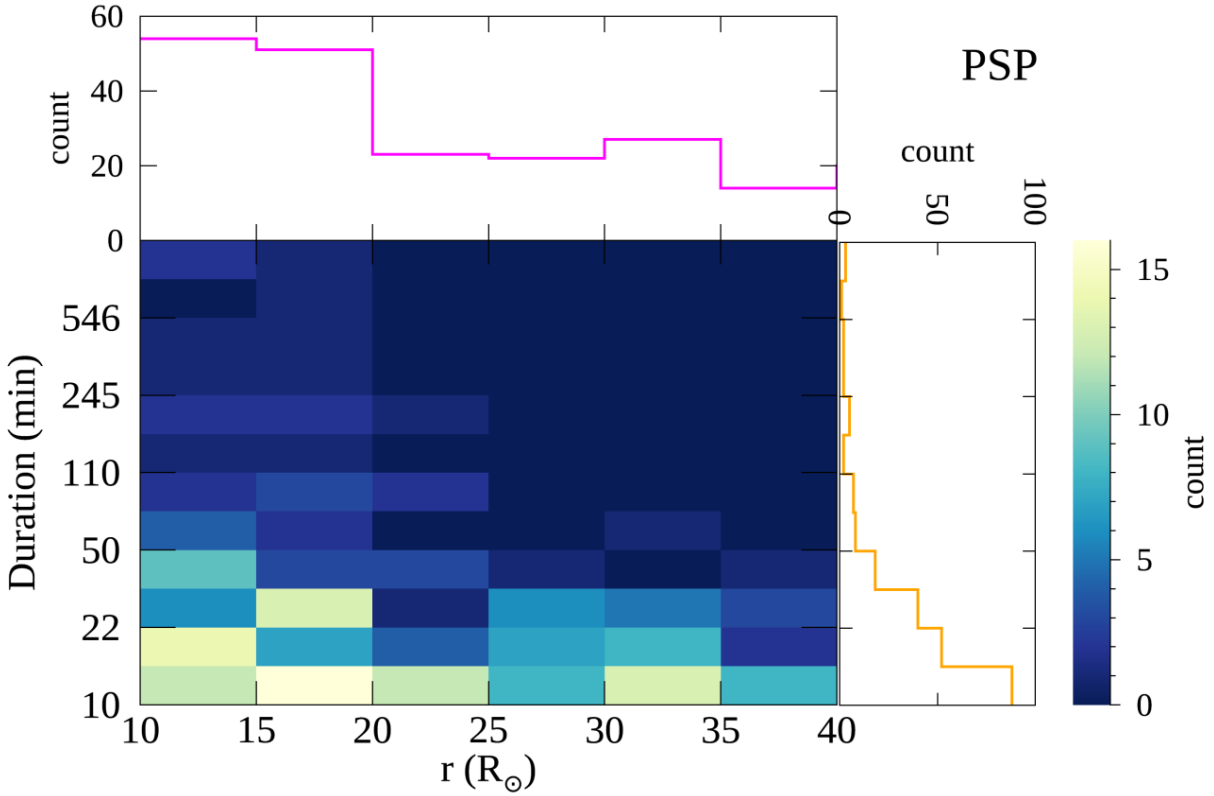

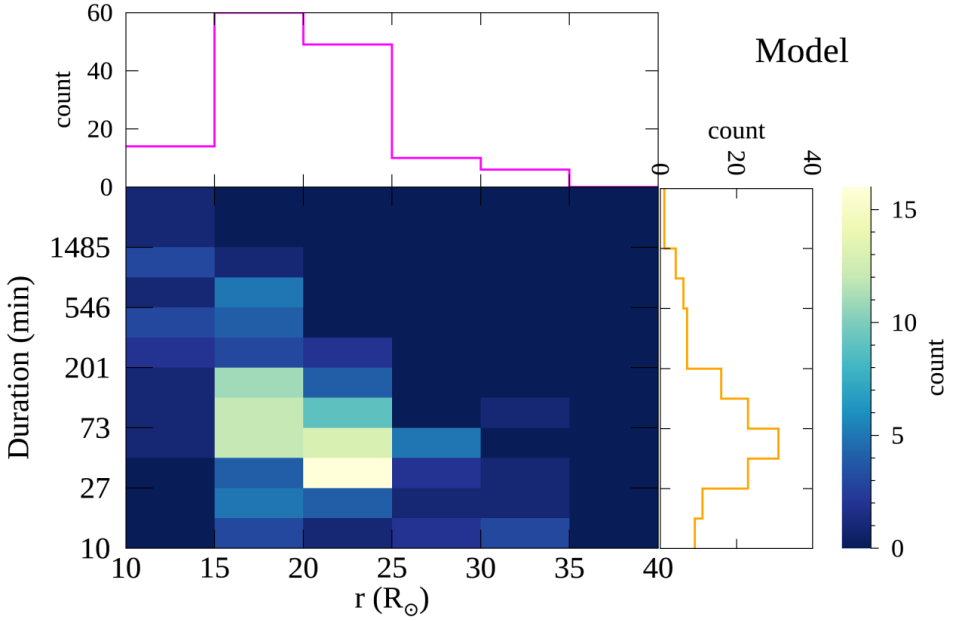

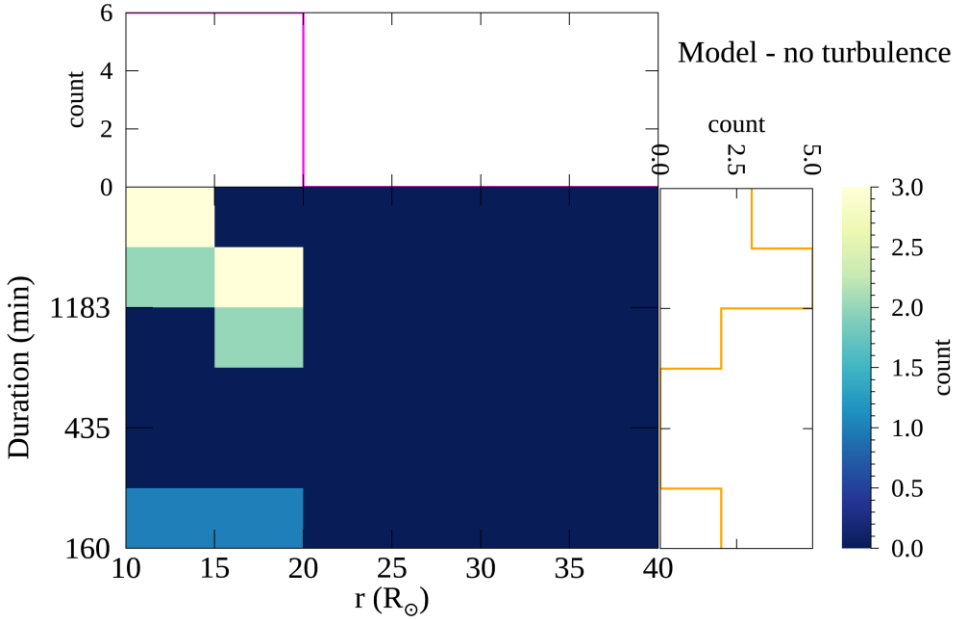

Chhiber+ 2024, *in prep*

M_A of subAlfvenic intervals

Chhiber+ 2024, *in prep*

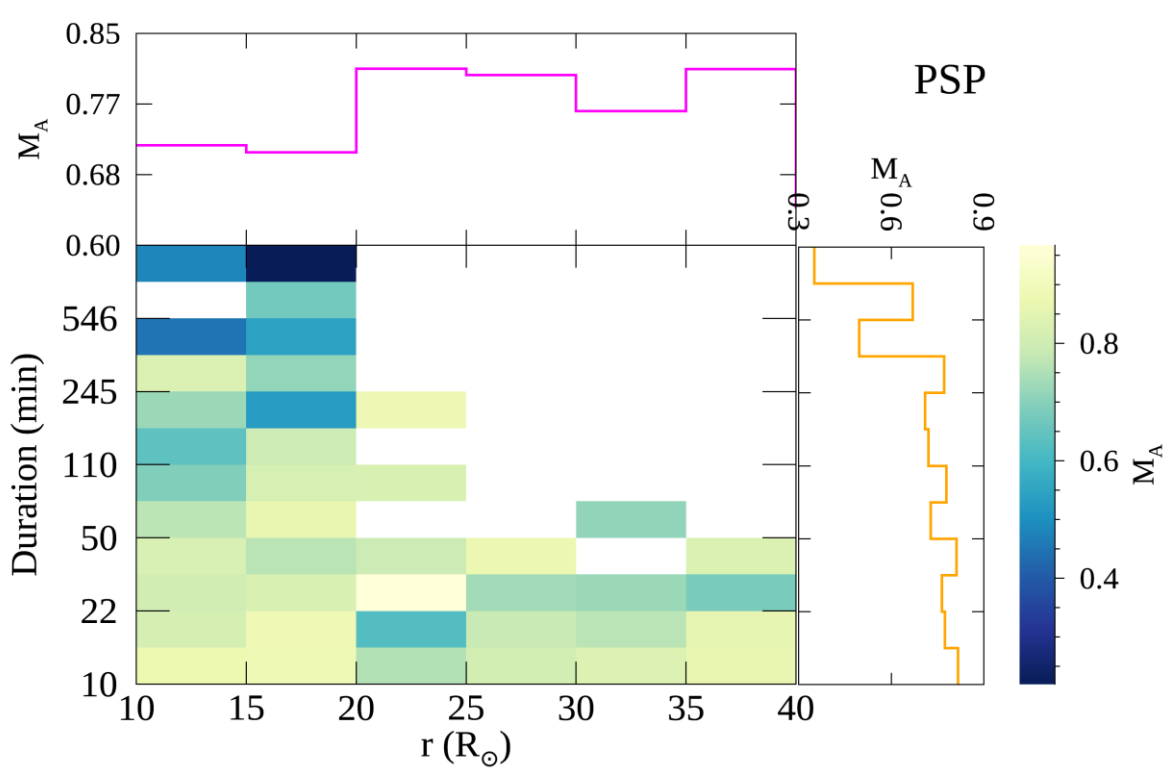

PSP

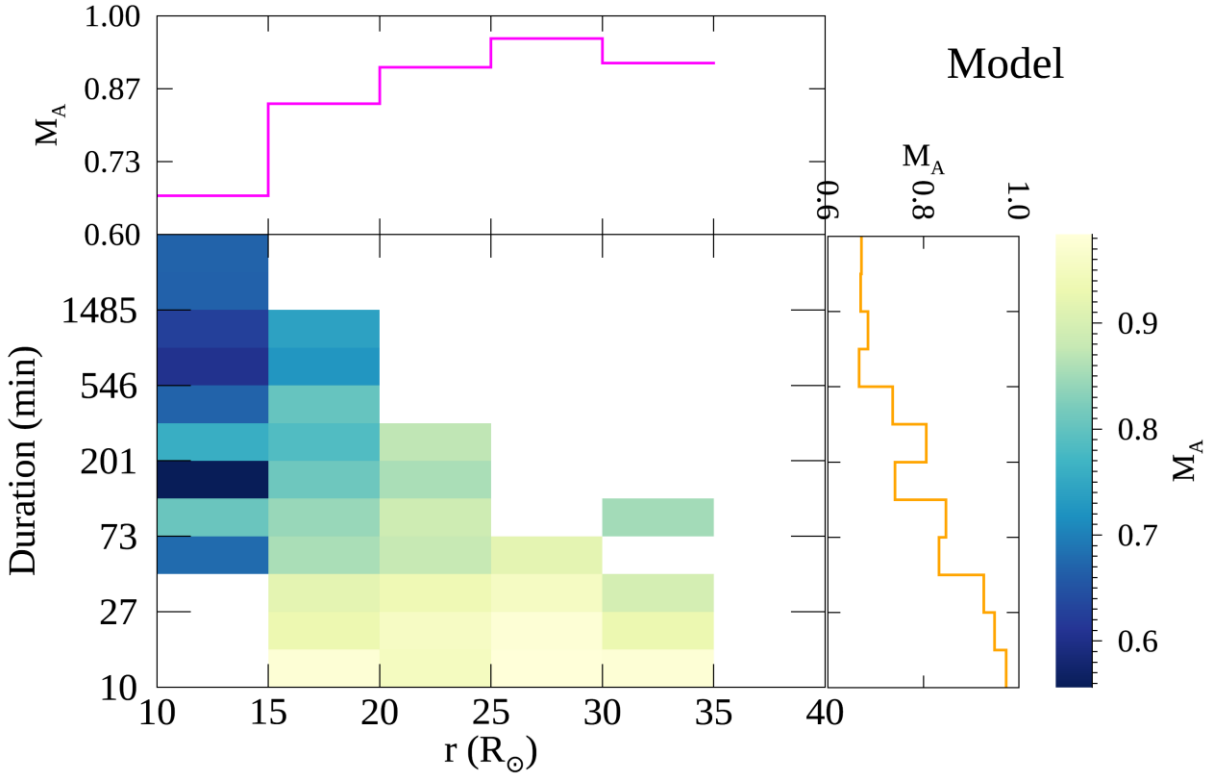

Model

“Bubble plots” of subAlfvenic interval duration

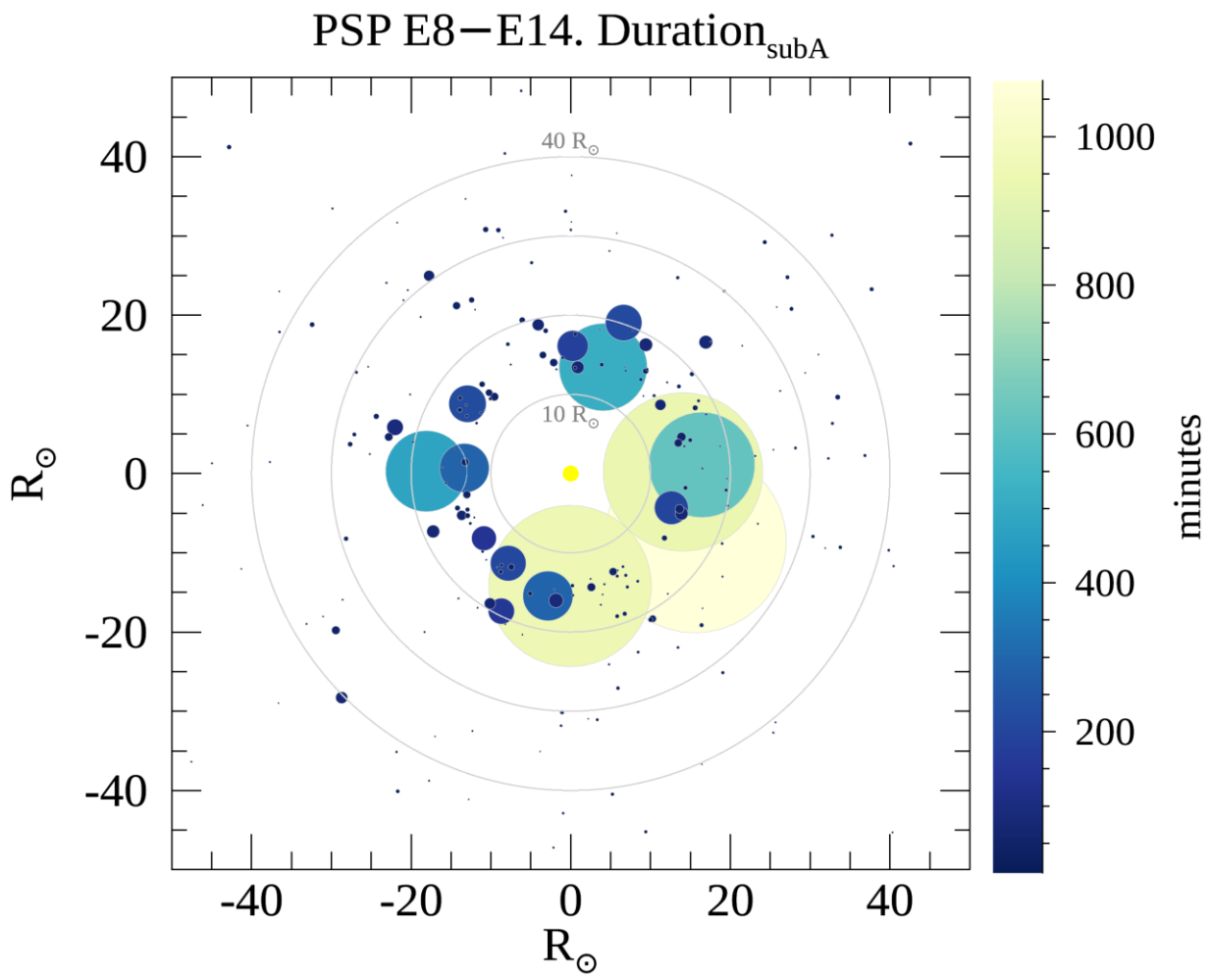

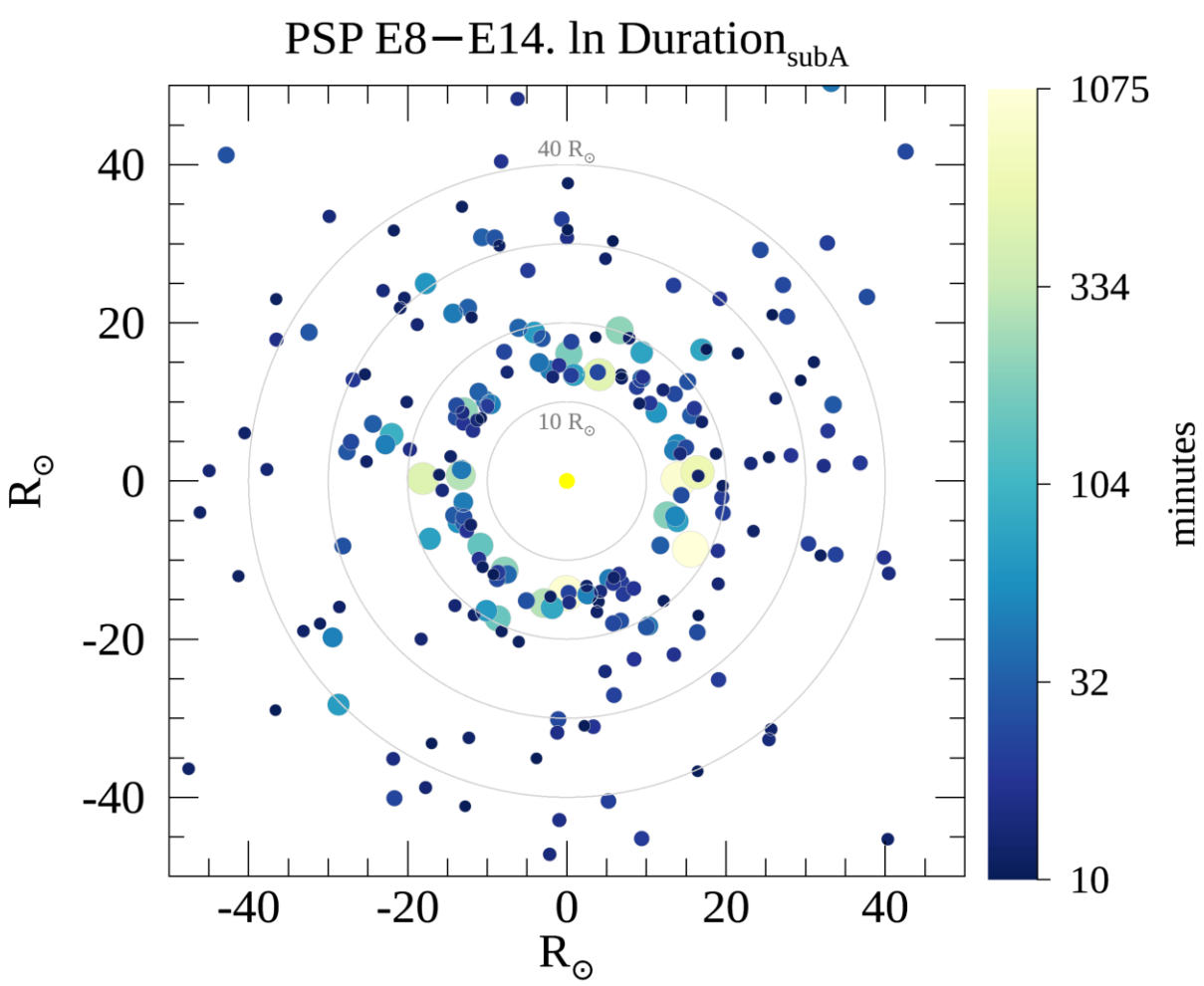

- Heliolongitude of intervals randomized
- Circle Diameter represents [*left*:] interval duration [*right*:] log (duration)
- Colorbar shows interval duration

Global properties of Alfven zone

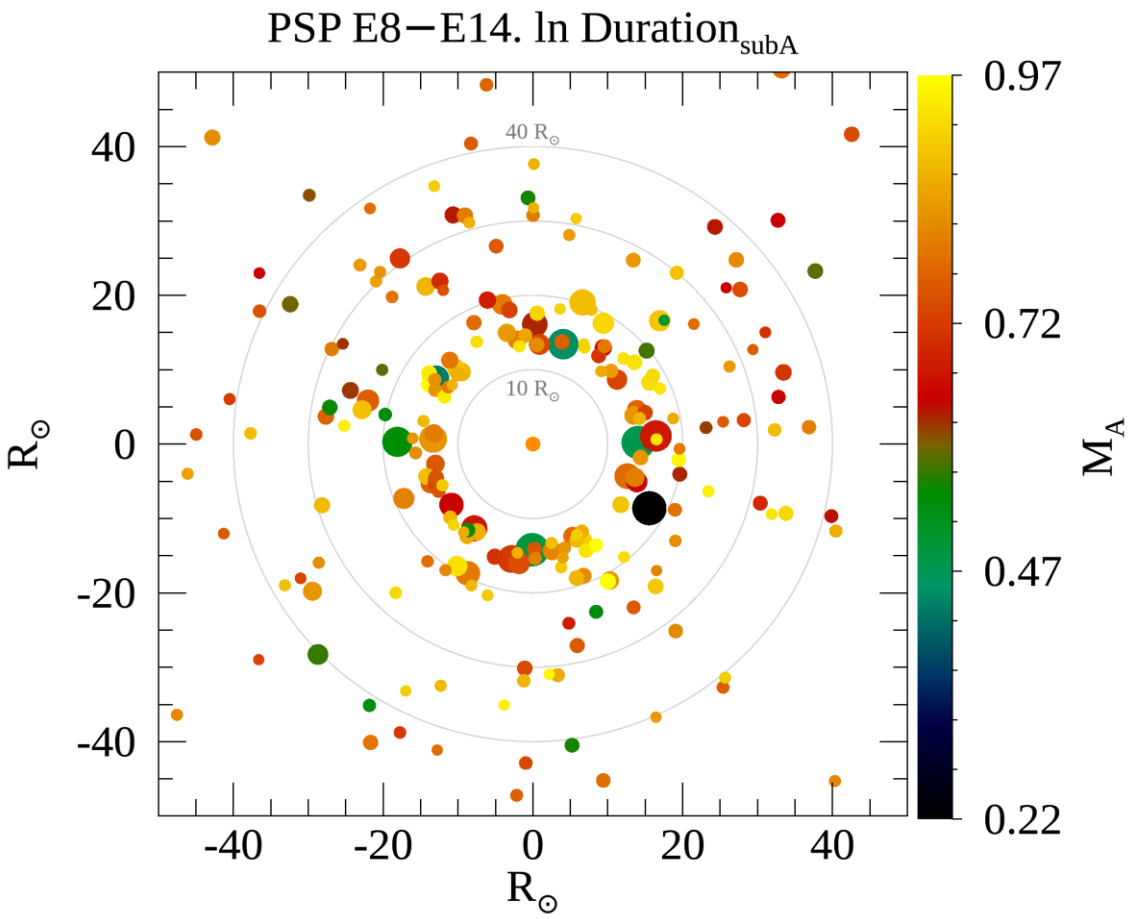

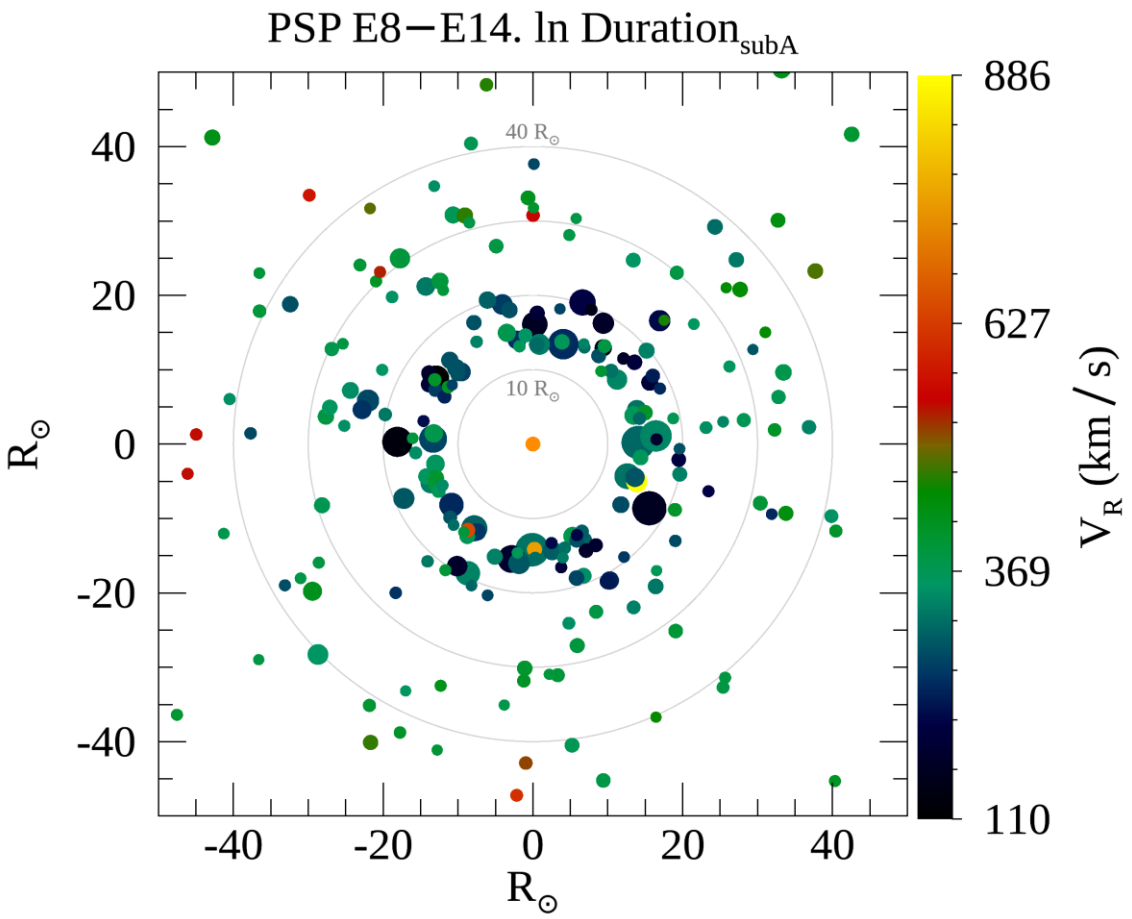

Global properties of Alfven zone

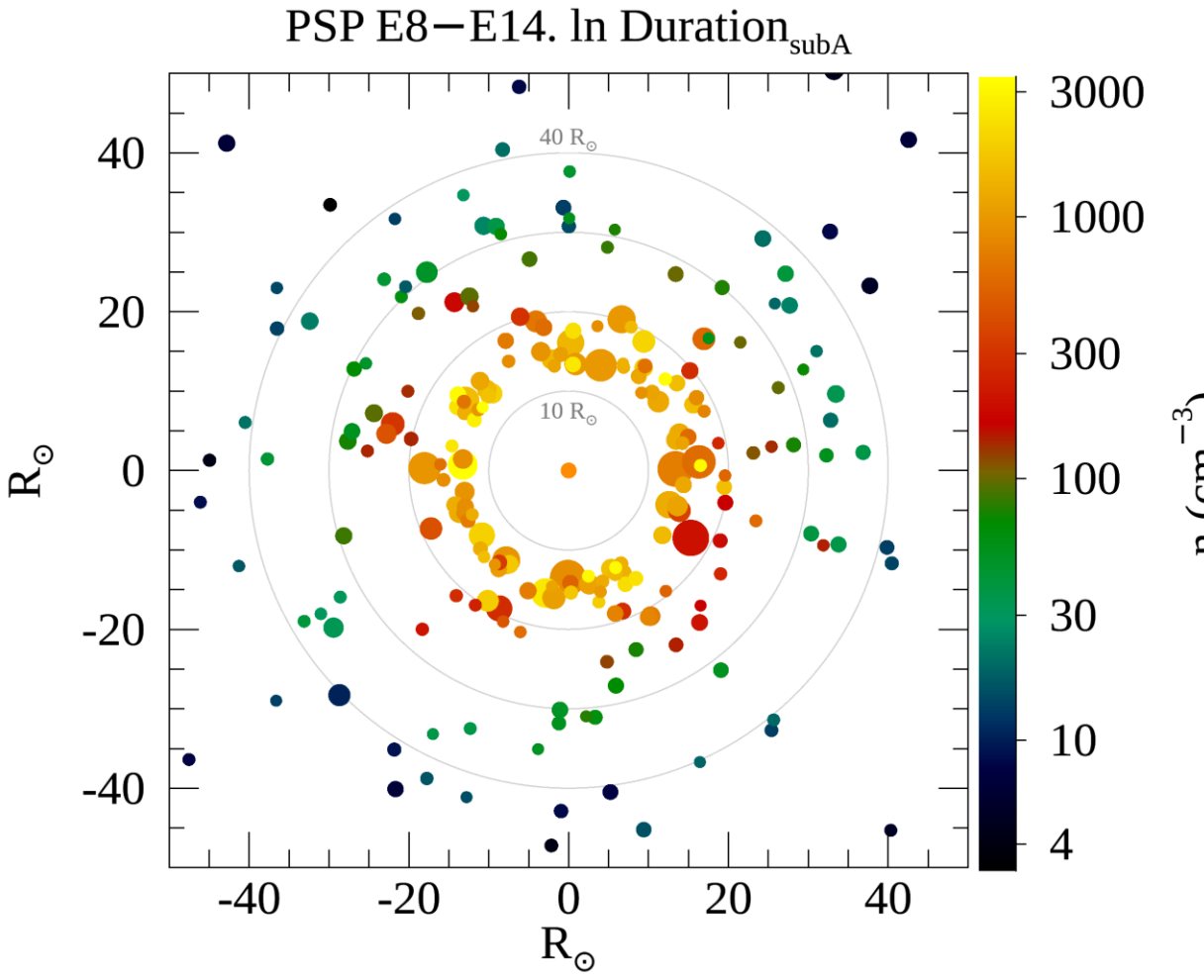

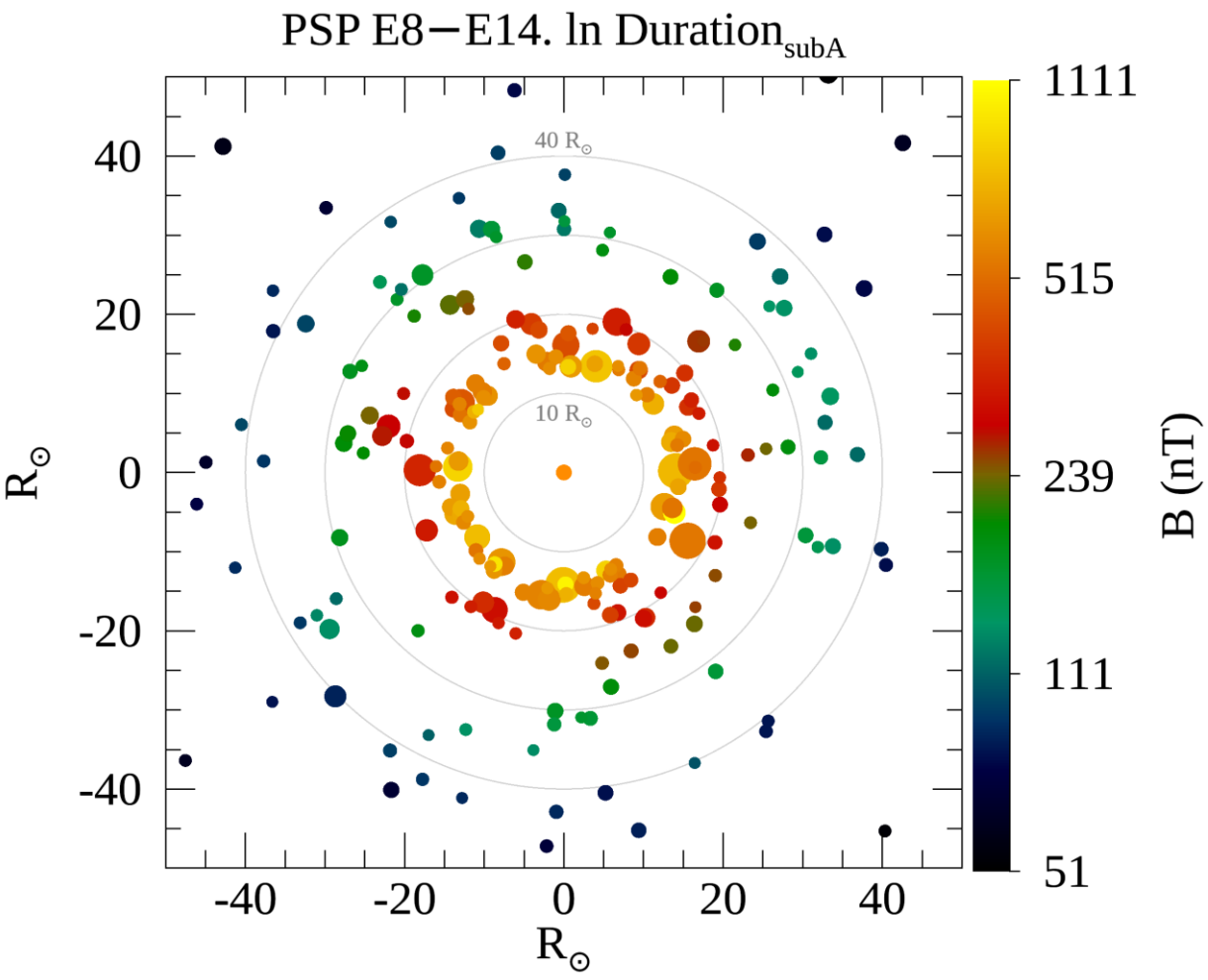

Outline

- Introduction and overview of Alfvén surface
- Turbulence; Extended and fragmented Alfvén zone in global model
- Global properties of Alfvén zone from Parker Solar Probe observations and model
- Stochastic propagation of Alfvén waves in the Alfvén zone
- Conclusions

PUNCH mission – Mapping the Alfven Zone

- Polarimeter to UNify the Corona and Heliosphere - https://punch.space.swri.edu/
- Constellation of four small satellites in Sun-synchronous, low-Earth orbit; produce deep-field, continuous, 3D images of solar corona as it makes a transition to the young solar wind ($6 - 180\ R_{\odot}$)
- Science Objective 1C: Alfvén Zone: Boundary of the Heliosphere. Map the evolution of the Alfvén zone by measuring inbound vs. outbound features in image sequences

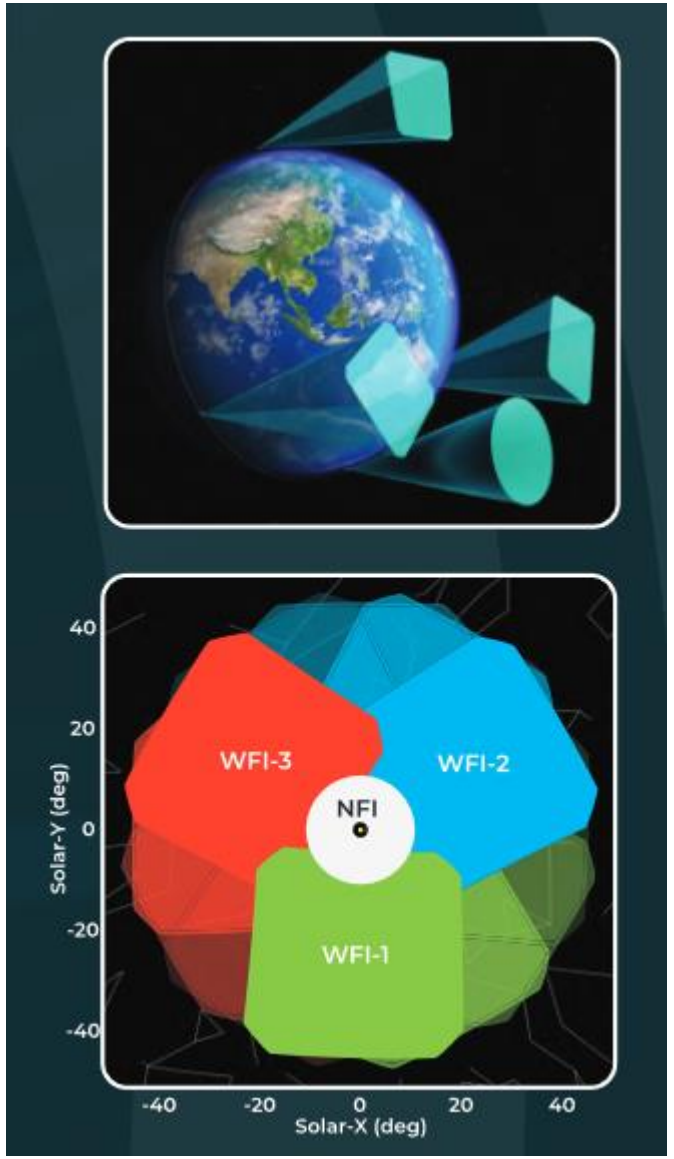

Stochastic trajectories of sunward propagating Alfvenic signals

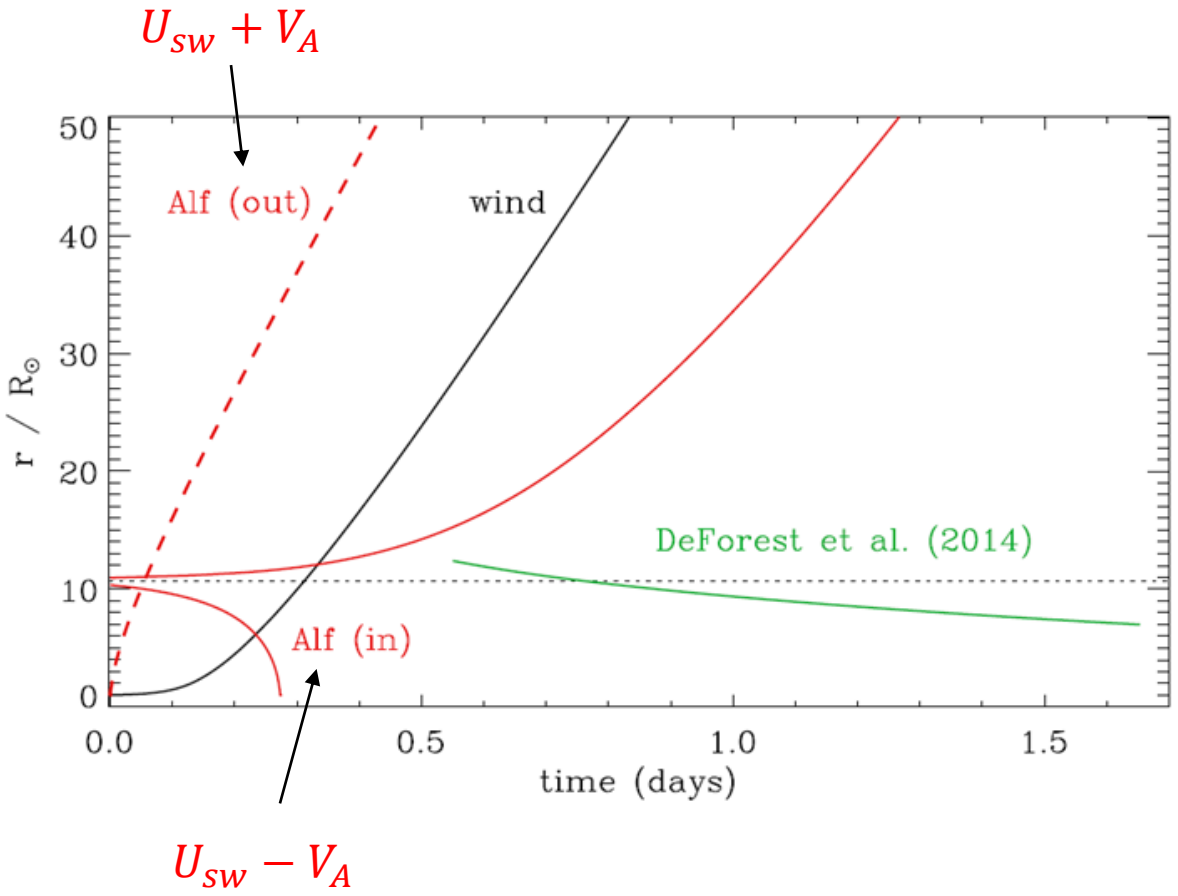

Cranmer+ 2023, Sol Phys

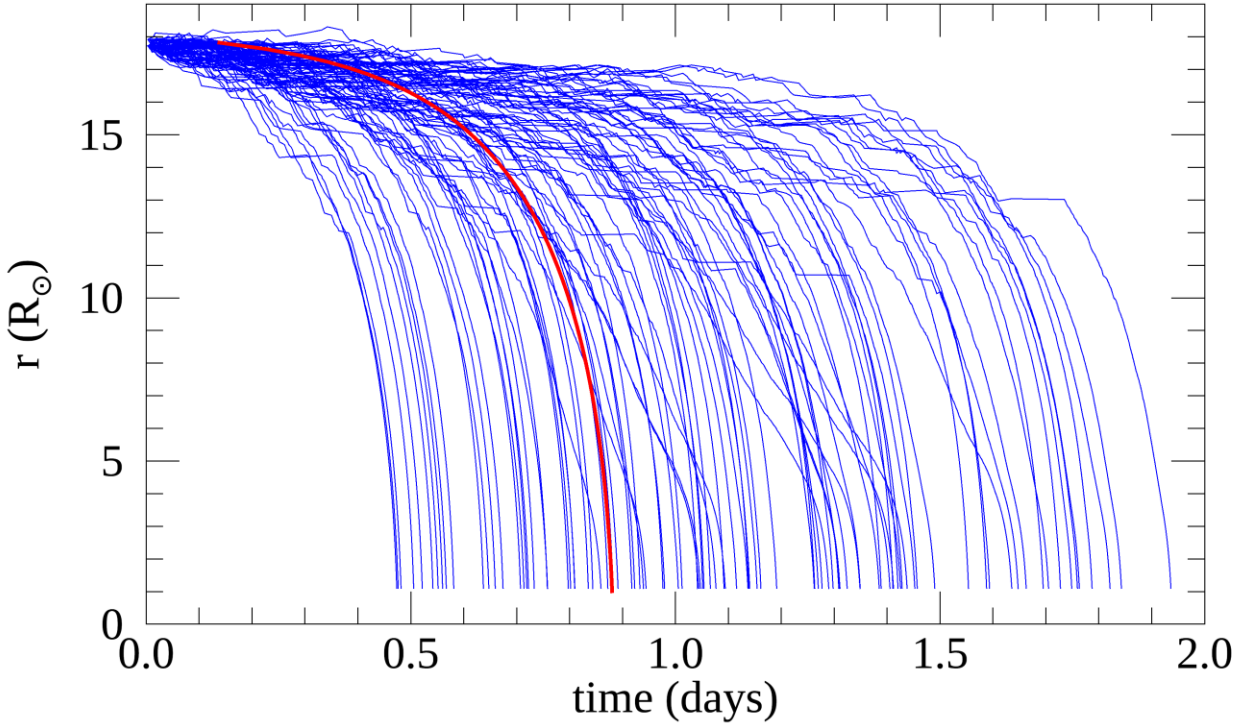

- Speed of signals = $U_{sw} - V_A$
- Red curve shows trajectory without turbulence

Conclusions & Discussion

- Turbulence implies an extended spatial region of transition from subAlfvenic to superAlfvenic flow, occurring in disconnected blobs
- 3D global simulations with turbulence modeling are a useful tool to examine these effects
- PSP observations consistent with fragmented Alfven zone covering a range of helioradii
- Alfvenic signals exhibit a prolonged stochastic motion while “trapped” in Alfven zone
- Enhanced heating/dissipation; nonlinear interactions of inward and outward propagating modes; enhanced SEP scattering…

Future Work

- Include both velocity and magnetic (density..) fluctuations; cross-helicity effects could produce more inhomogeneous distributions of patches
- Comparison of subAlfvenic and superalfvenic intervals (see also Bandyopadhyay+ 2022, ApJL)

Extra Slides

Effect of velocity fluctuations and v-b correlations

No v fluctuations

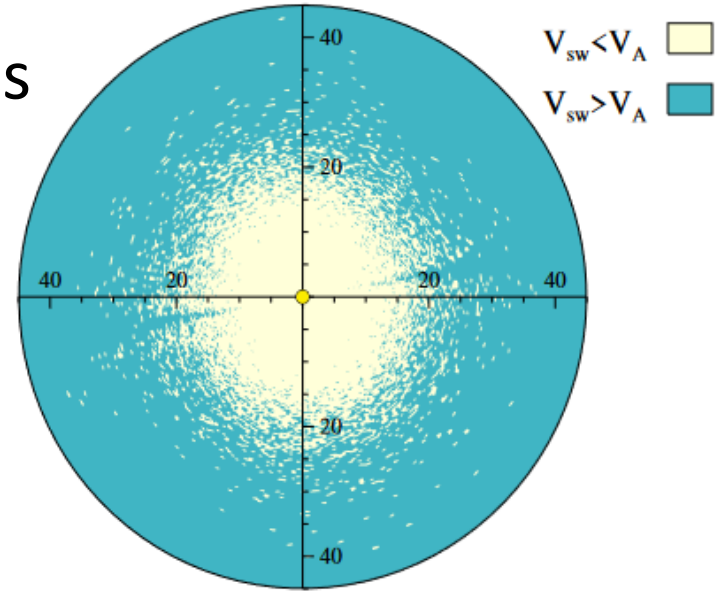

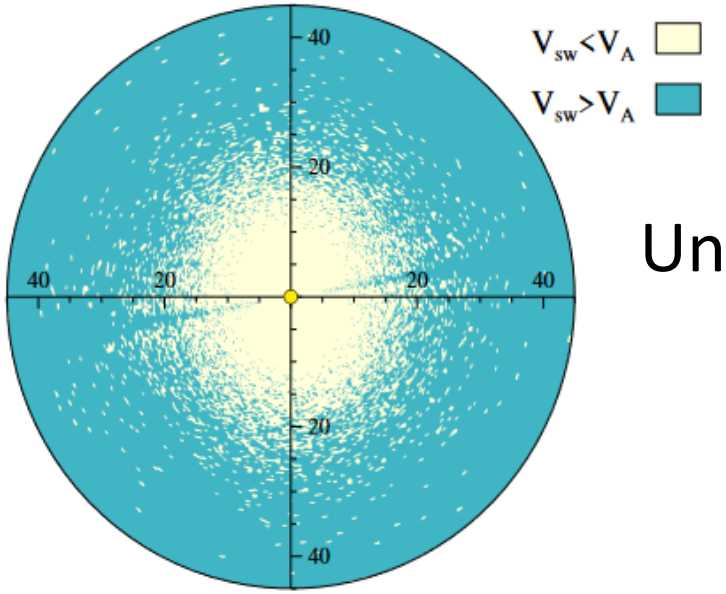

Uncorrelated v-b

Correlated v-b (based on σ_c from model)

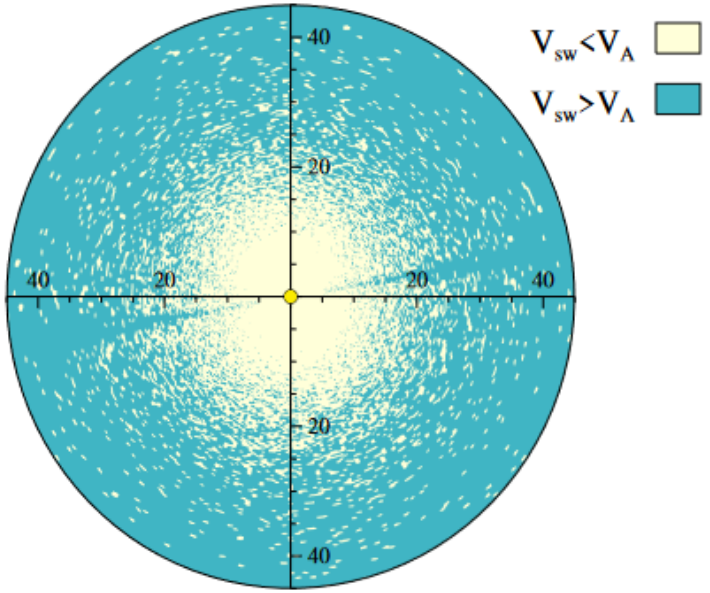

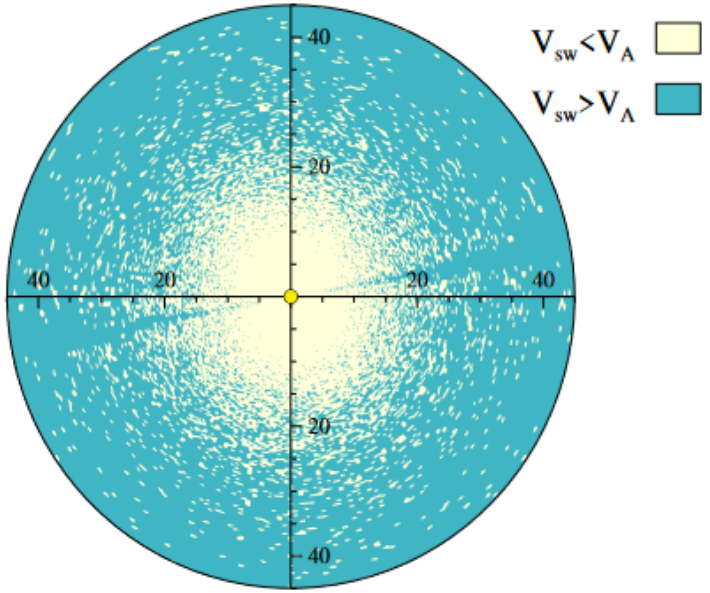

Flows in and around the Alfven zone

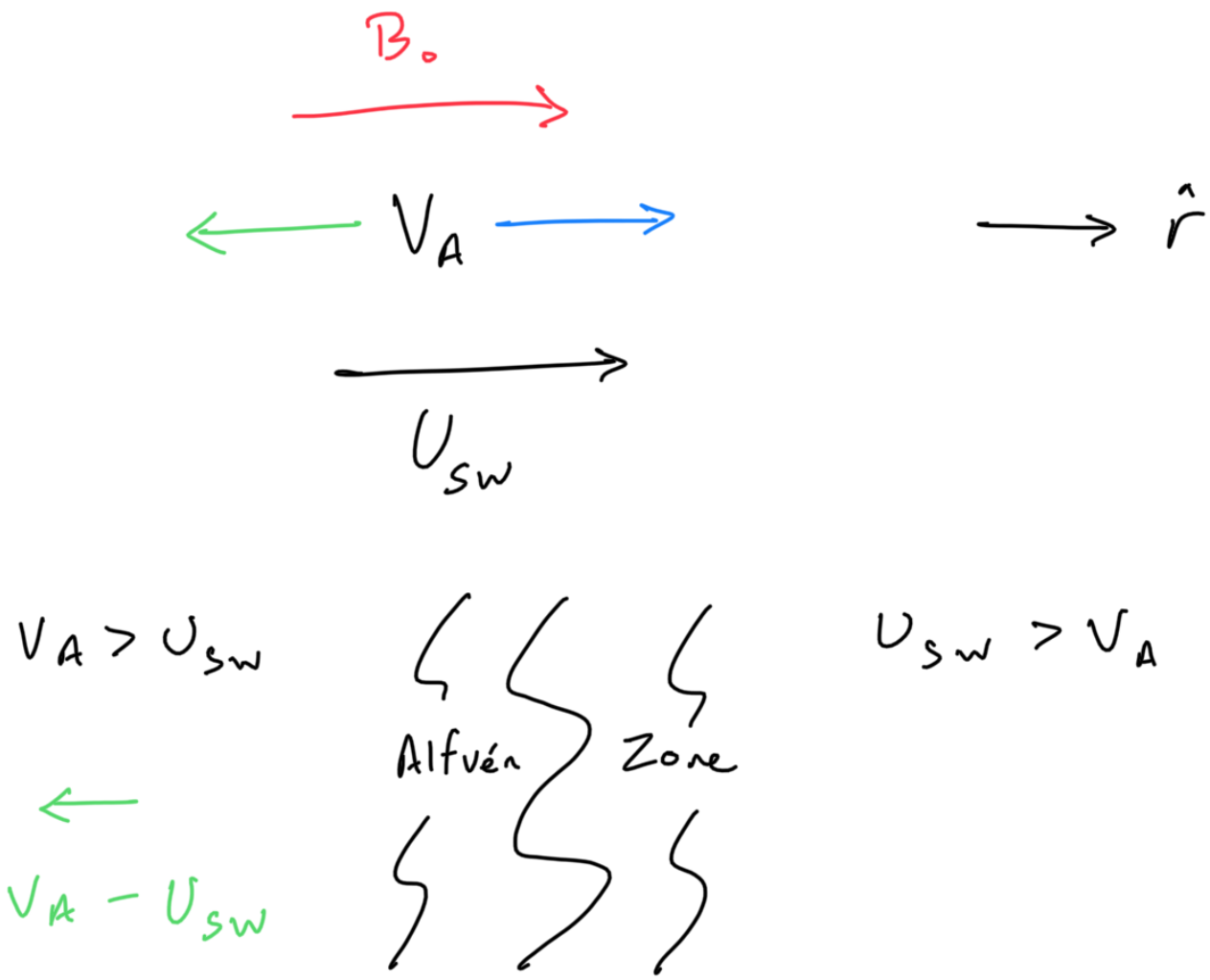

Stochastic trajectories of sunward propagating Alfvenic signals

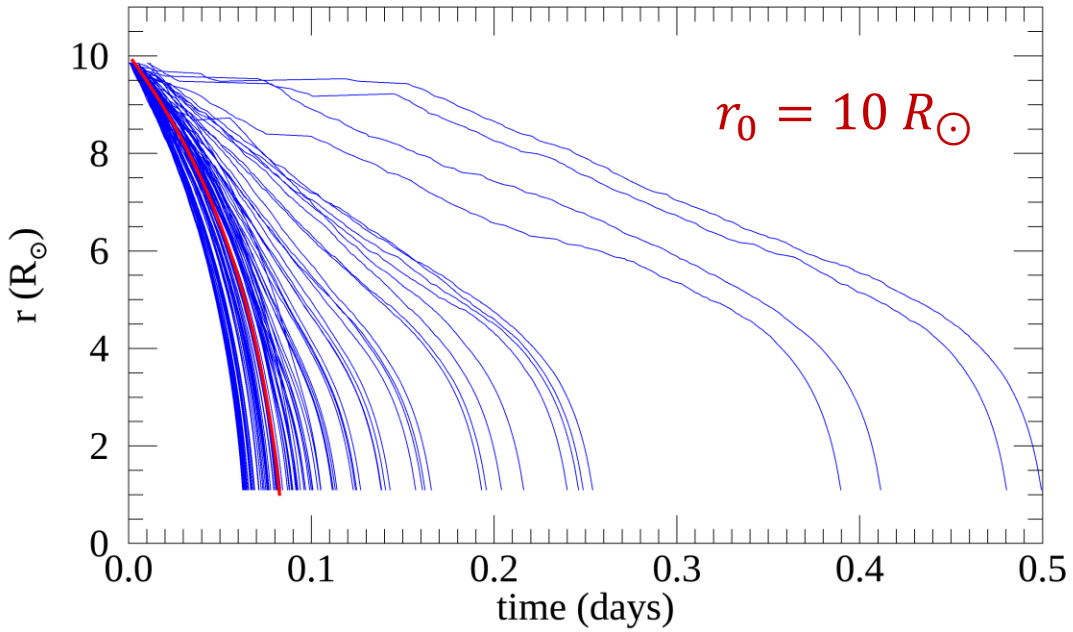

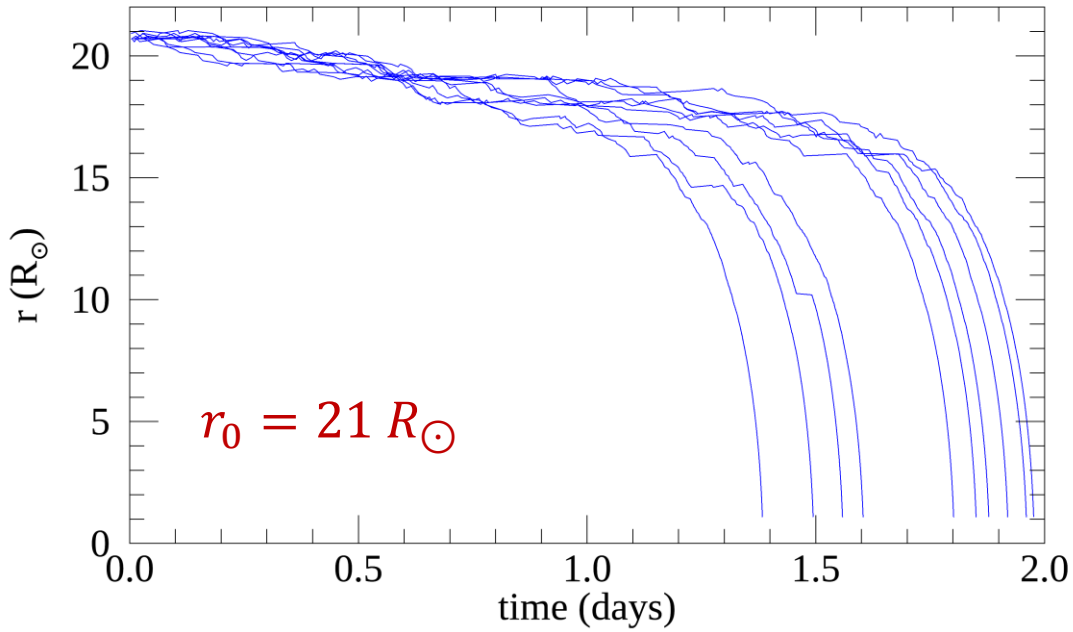

- Speed of signals = $V_A - U_{sw}$
- Red curve shows trajectory without turbulence

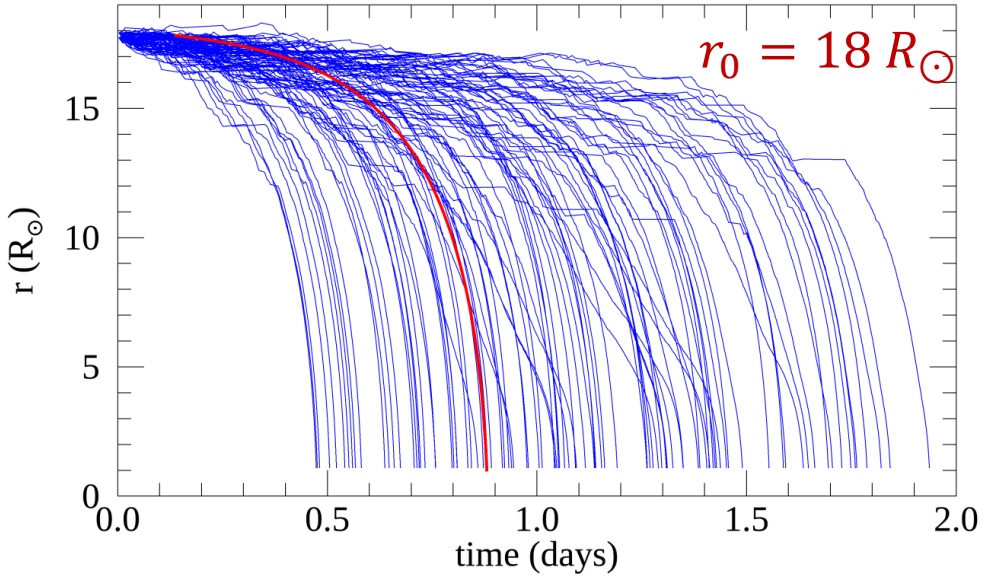

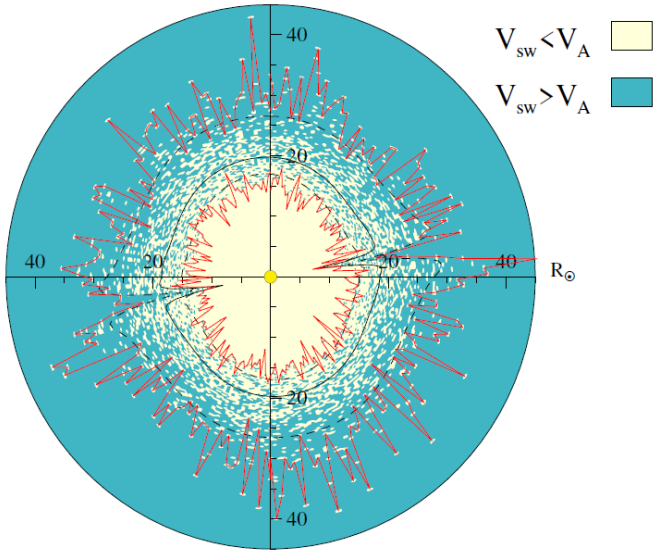

Stochastic trajectories of sunward propagating Alfvenic signals

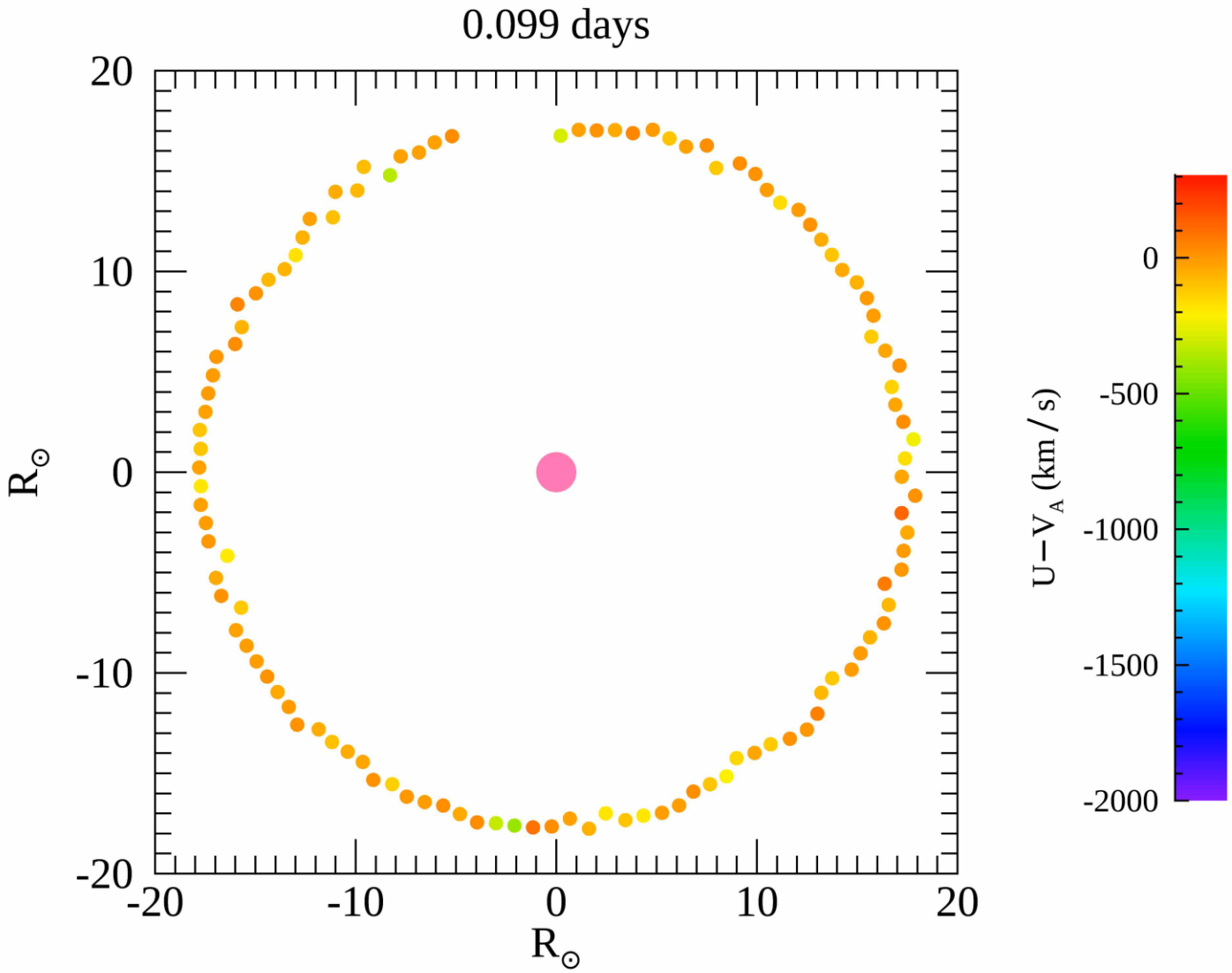

https://www.youtube.com/watch?v=EPgvfAi4uV8

Alfven speeds of sub and super-Alfvenic patches

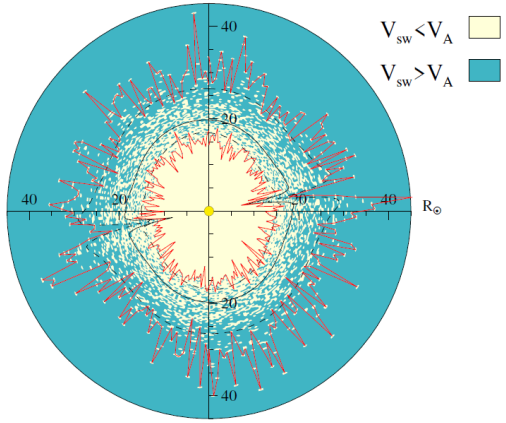

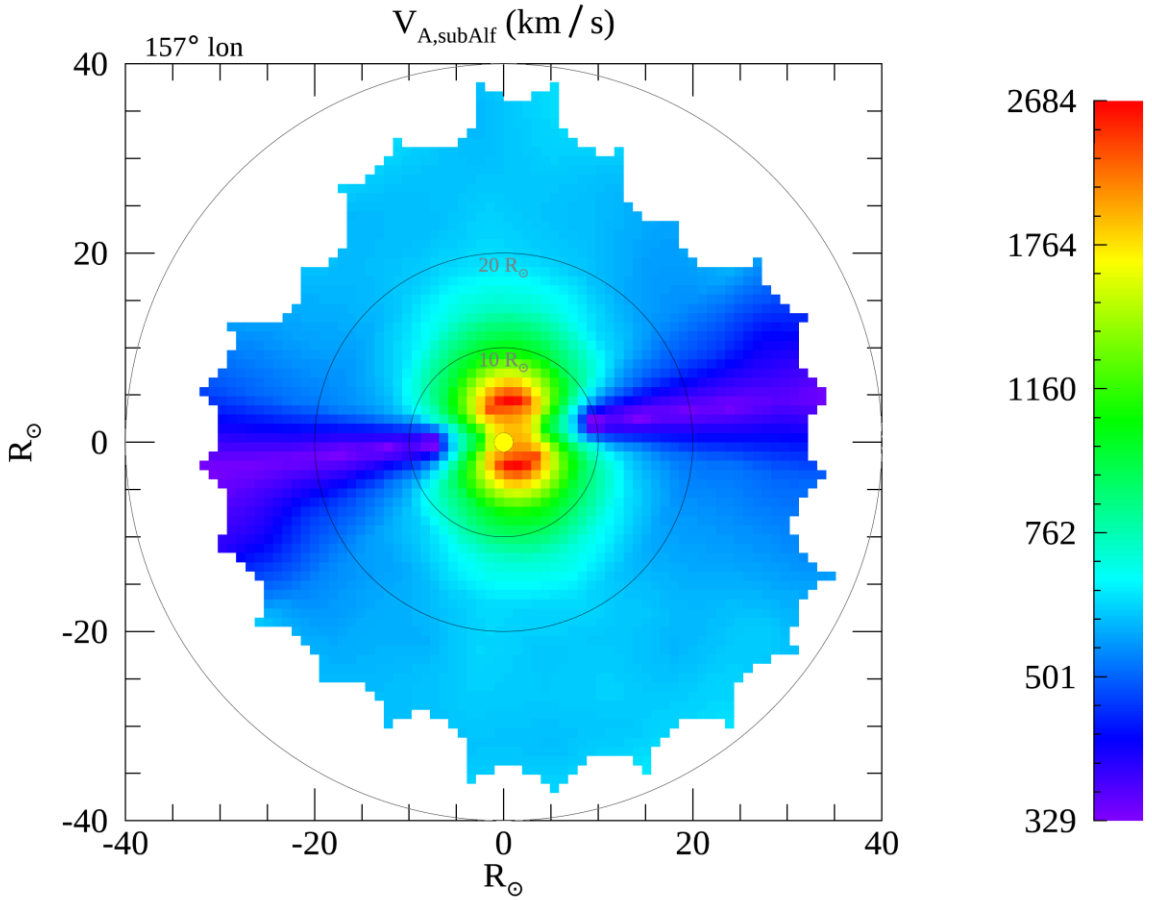

$V_{\mathrm{A,sub-Alfvenic}}$ (km/s)

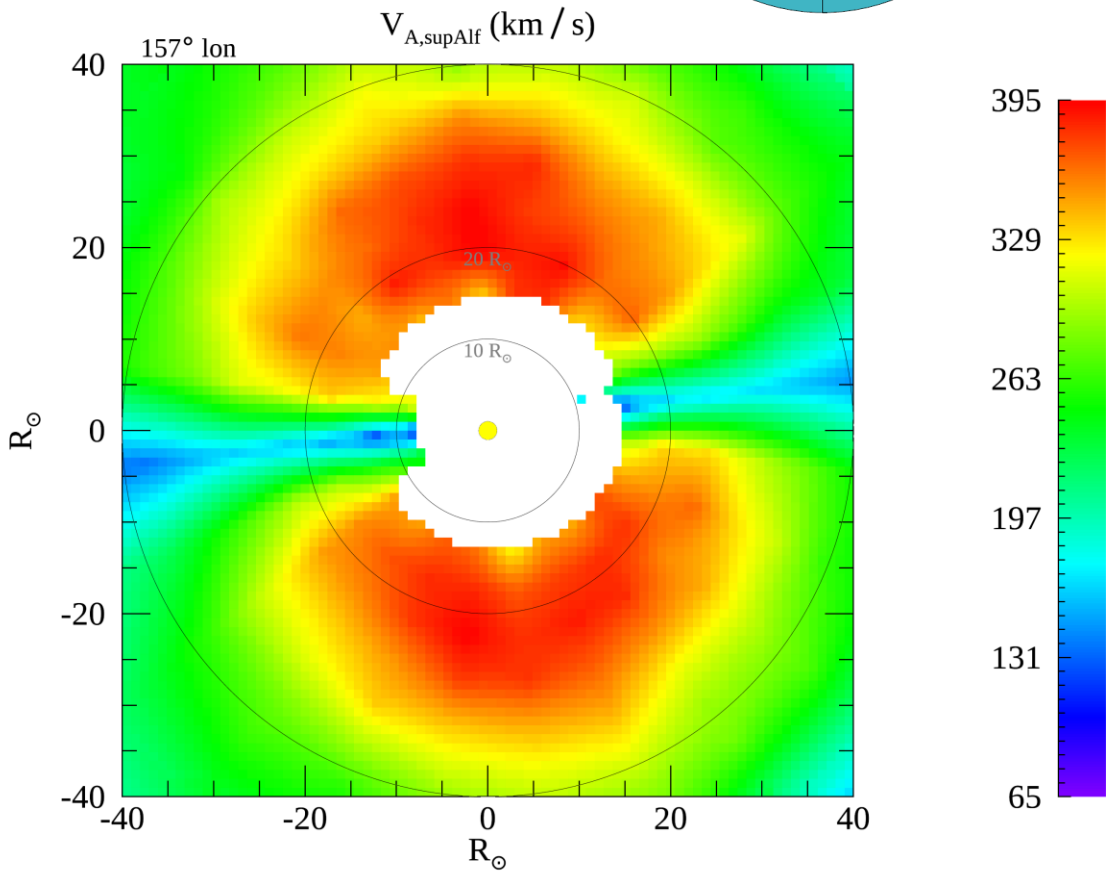

$V_{\mathrm{A,super-Alfvenic}}$

Anti-sunward propagation speeds

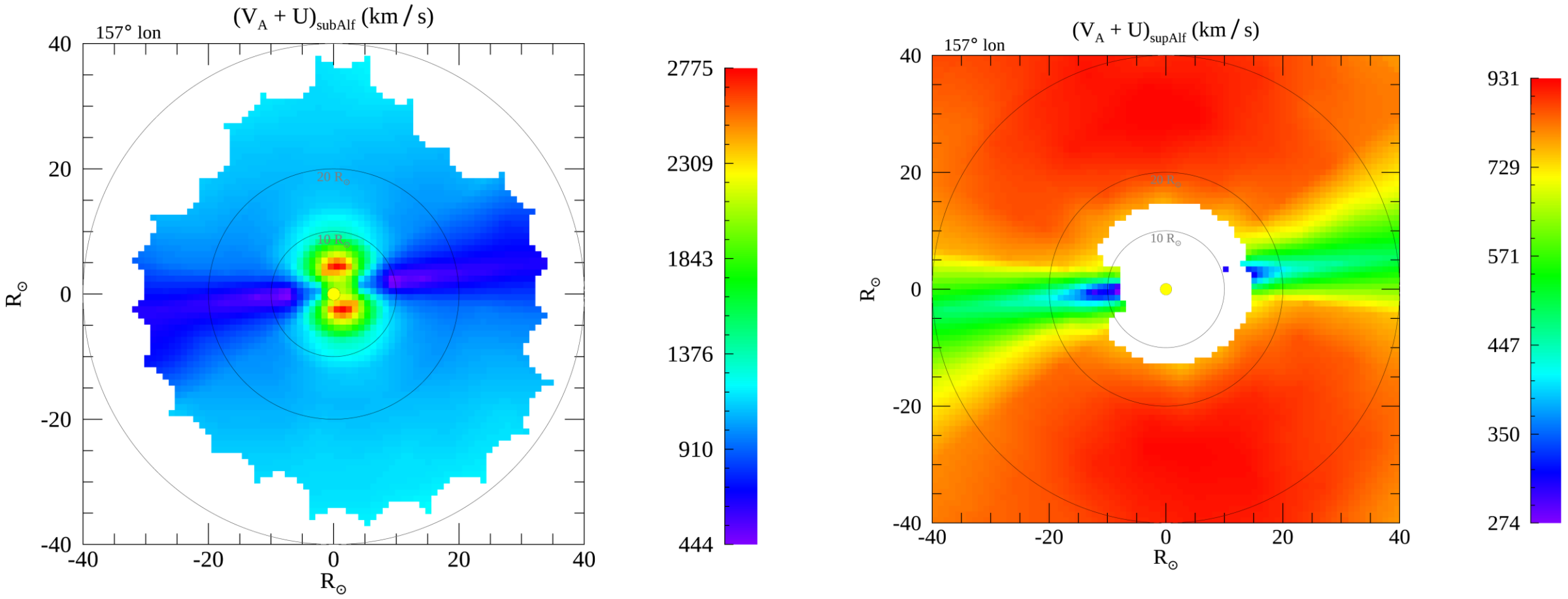

$(V_A + U_{sw})_{\text{subAlfvenic}}$ (km/s) $(V_A + U_{sw})_{\text{superAlfvenic}}$

Sunward propagation speeds of sub-Alfvenic fluctuations

$(V_A - U_{sw})_{\text{subAlfvenic}}$ (km/s)

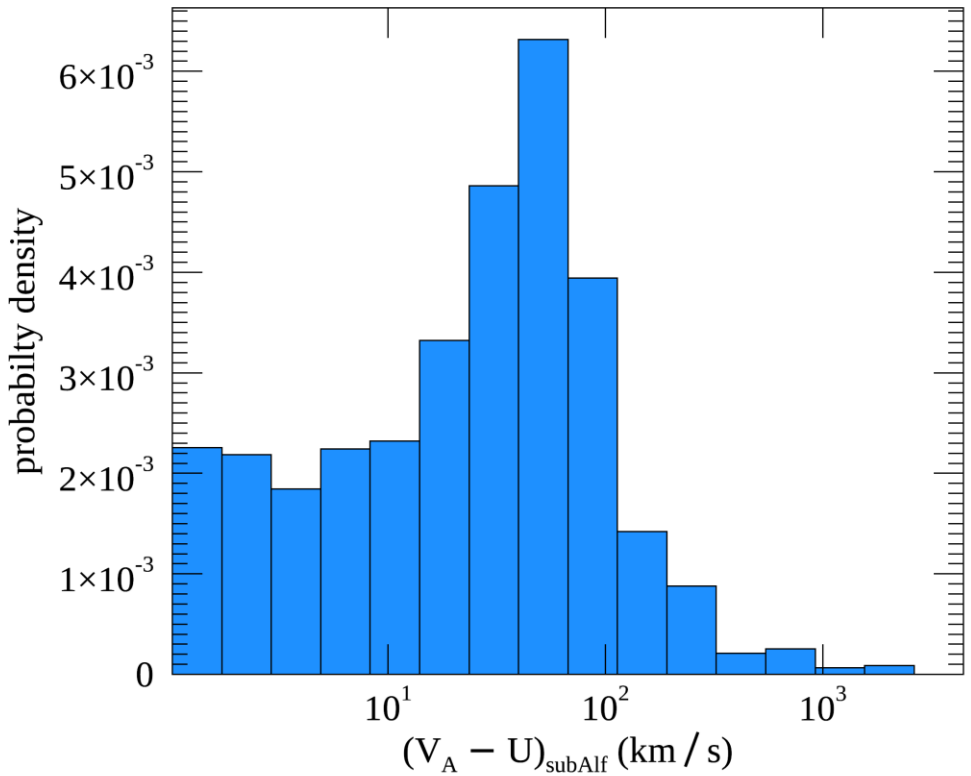

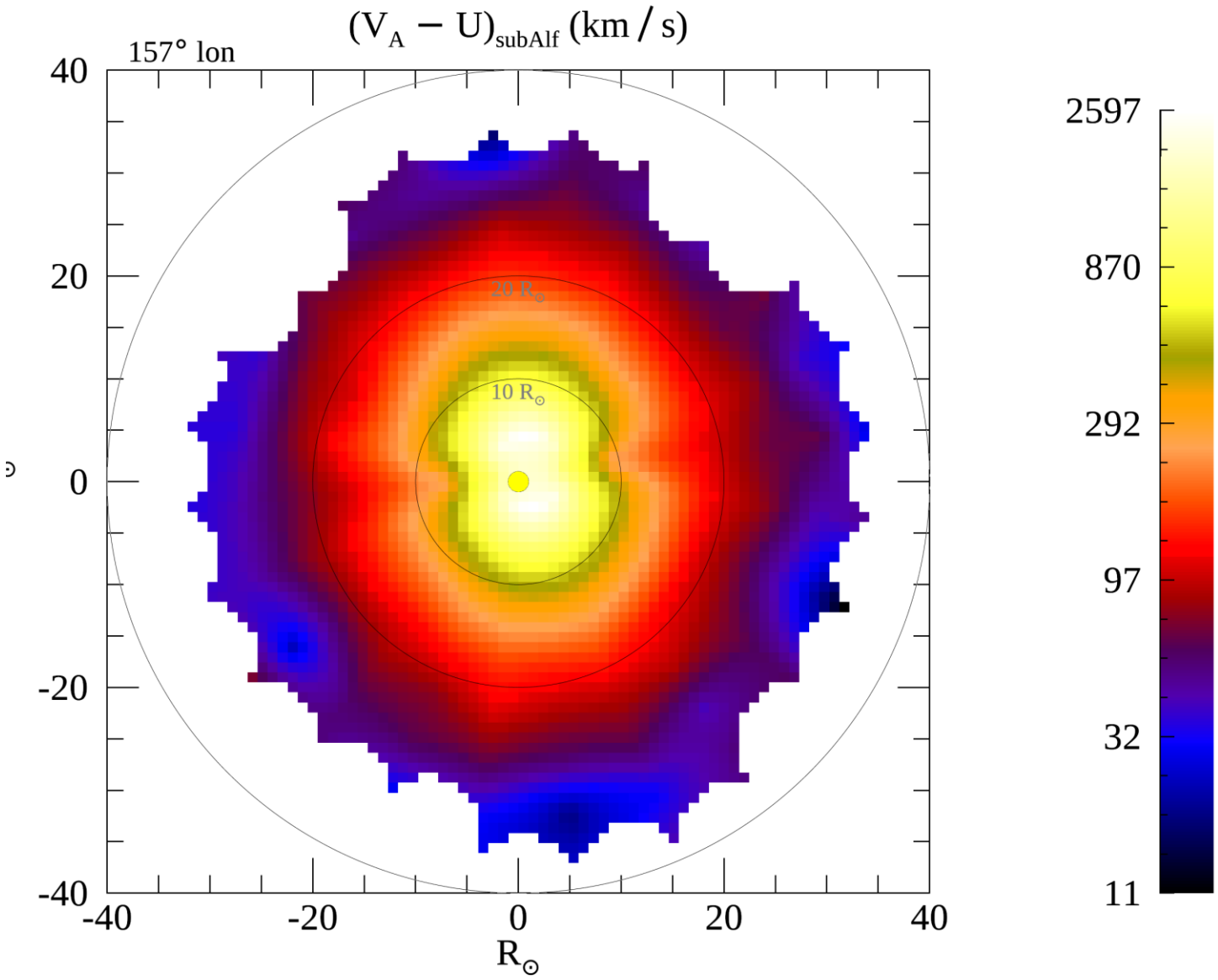

Spatial scales of sub-Alfvenic patches – variation in longitude

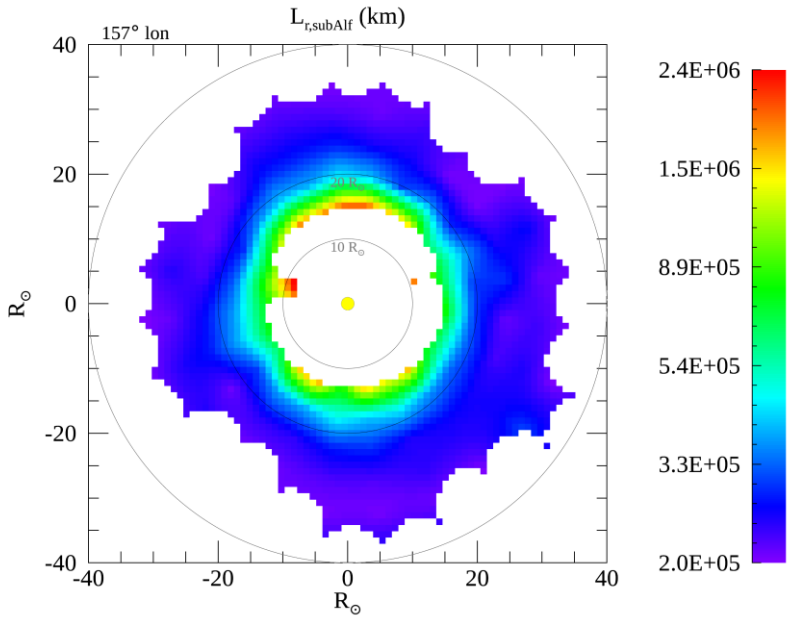

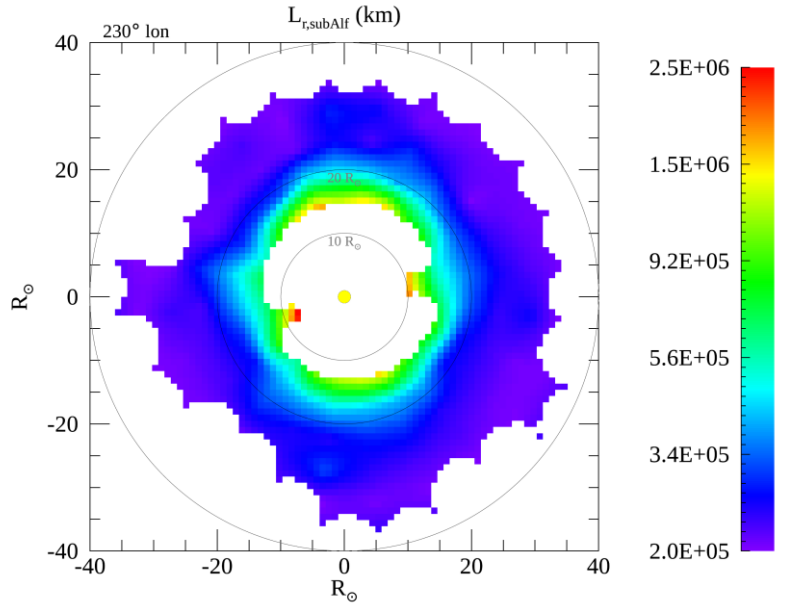

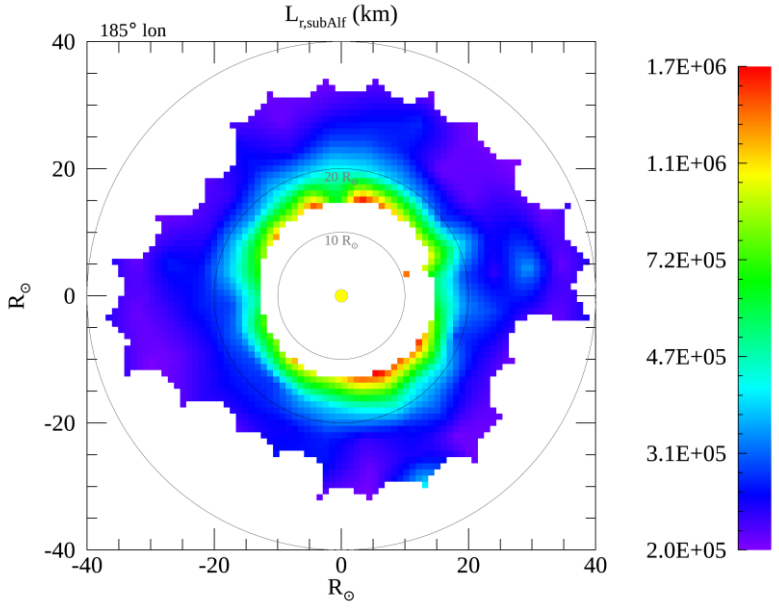

PDF of spatial scales across all longitudes

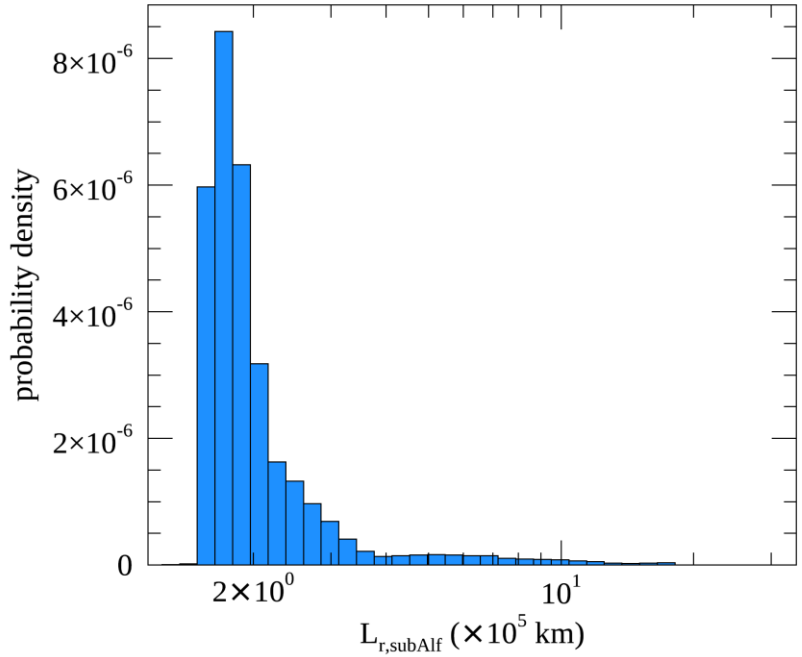

Turbulence compared between subAlfvenic and superAlfvenic intervals (PSP)

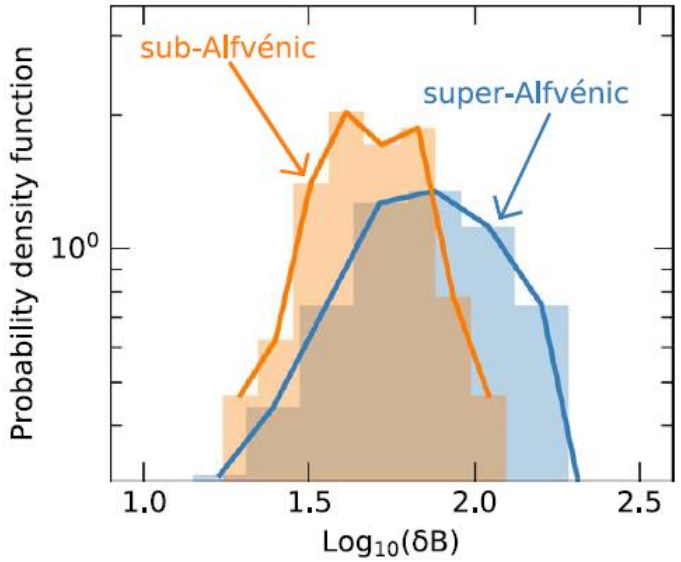

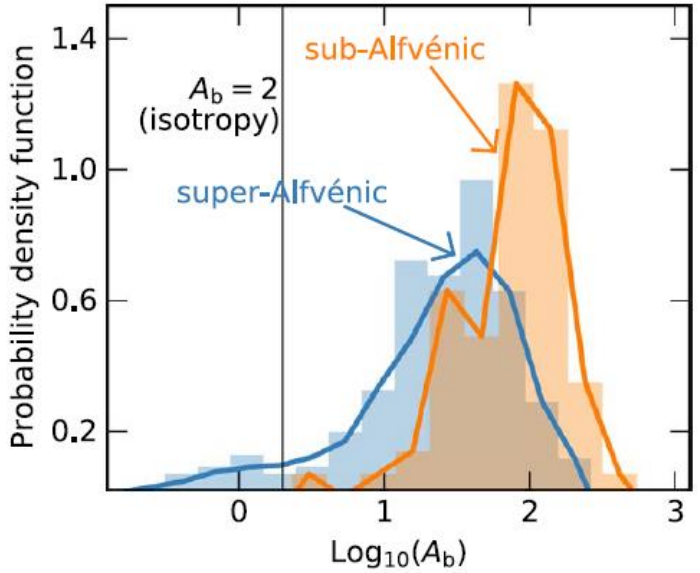

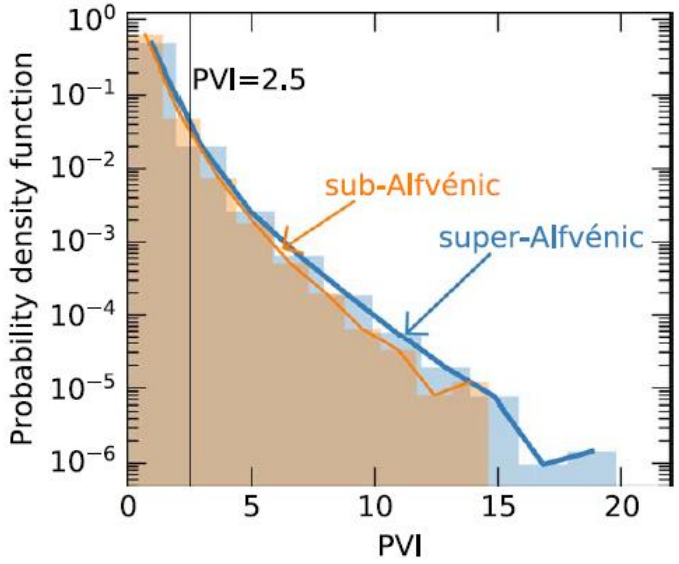

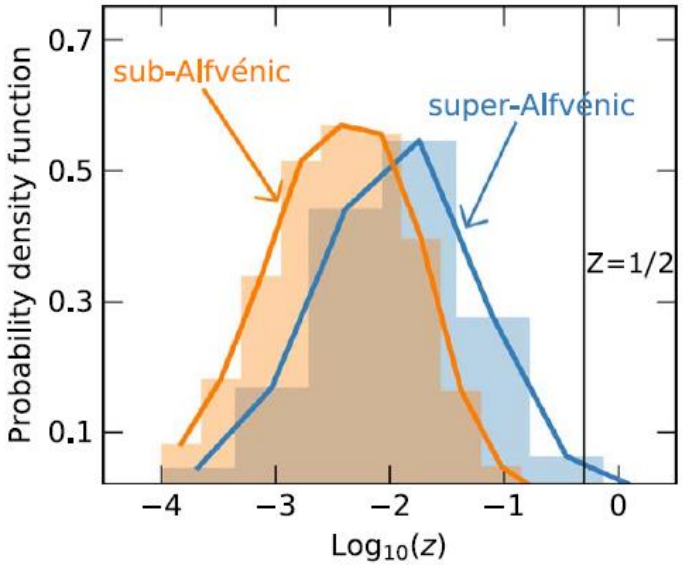

Clockwise from top left – fluctuation amplitude, variance anisotropy, intermittency (PVI), number of switchbacks

Bandyopadhyay+ 2022

Global sim w' turbulence modeling – Comparison with five PSP orbits

$$Z^2 = \langle v'^2 + b'^2 \rangle$$

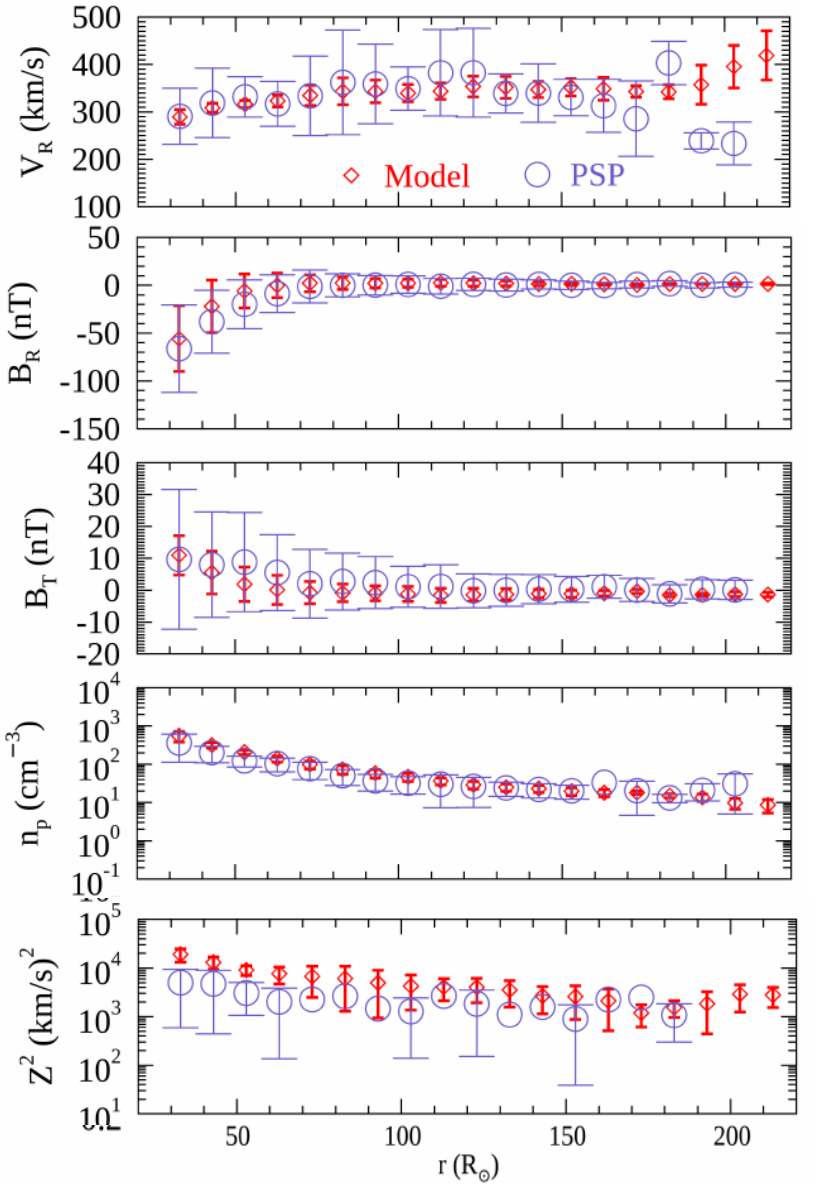

Chhiber+ 2021, ApJ

Two-Fluid Reynolds Averaged MHD Equations

$$\frac{\partial \rho}{\partial t} + \nabla \cdot (\rho \mathbf{v}) = 0$$

$$\frac{\partial(\rho \mathbf{u})}{\partial t} + \nabla \cdot \left[\rho \mathbf{v}\mathbf{u} - \frac{1}{4\pi}\mathbf{B}\mathbf{B} + \left(P_S + P_E + \frac{B^2}{8\pi} + \frac{\langle B'^2 \rangle}{8\pi} \right) \mathbf{I} + \boldsymbol{\mathcal{R}} \right] = -\rho \left(\frac{GM_\odot}{r^2} + \boldsymbol{\Omega} \times \mathbf{u} \right)$$

$$\frac{\partial \mathbf{B}}{\partial t} = \nabla \times (\mathbf{v} \times \mathbf{B} + \varepsilon_m \sqrt{4\pi\rho})$$

$$\frac{\partial P_S}{\partial t} + (\mathbf{v} \cdot \nabla) P_S + \gamma P_S \nabla \cdot \mathbf{u} + (\gamma - 1) \frac{P_S - P_E}{\tau_{SE}} = f_p Q_T$$

$$\frac{\partial P_E}{\partial t} + (\mathbf{v} \cdot \nabla) P_E + \gamma P_E \nabla \cdot \mathbf{u} + (\gamma - 1) \left[\frac{P_E - P_S}{\tau_{SE}} + \nabla \cdot \mathbf{q}_H \right] = (1 - f_p) Q_T$$

- P_S and P_E are the proton and electron pressure
- $\mathbf{u}$ is the velocity in the inertial frame
- $\mathbf{v}$ is the velocity in the rotating frame
- τ_{SE} is the electron-proton Coulomb collision rate
- $\boldsymbol{\mathcal{R}} = \langle \rho \mathbf{v}' \mathbf{v}' - \frac{\mathbf{B}'\mathbf{B}'}{4\pi} \rangle$ is the Reynolds stress tensor
- $\varepsilon_m = \frac{\langle \mathbf{v}' \times \mathbf{B}' \rangle}{(4\pi\rho)^{1/2}}$ is the mean turbulent electric field
- Q_T is the turbulent heating rate
- $\mathbf{q}_H$ is the electron heat flux

Two-Fluid Reynolds-averaged MHD with Turbulence Transport

- Turbulence transport equations obtained by subtracting mean-flow eqns. from full eqns., and averaging.

mean flow

$$\frac{\partial \rho}{\partial t} + \nabla \cdot (\rho \mathbf{v}) = 0$$

$$\frac{\partial (\rho \mathbf{u})}{\partial t} + \nabla \cdot \left[\rho \mathbf{v}\mathbf{u} - \frac{1}{4\pi}\mathbf{B}\mathbf{B} + \left(P_S + P_E + \frac{B^2}{8\pi} + \frac{\langle B'^2 \rangle}{8\pi} \right) \mathbf{I} + \boldsymbol{\mathcal{R}} \right] = -\rho \left(\frac{GM_\odot}{r^2} + \boldsymbol{\Omega} \times \mathbf{u} \right)$$

$$\frac{\partial \mathbf{B}}{\partial t} = \nabla \times (\mathbf{v} \times \mathbf{B} + \varepsilon_m \sqrt{4\pi\rho})$$

$$\frac{\partial P_S}{\partial t} + (\mathbf{v} \cdot \nabla) P_S + \gamma P_S \nabla \cdot \mathbf{u} + (\gamma - 1) \frac{P_S - P_E}{\tau_{SE}} = f_p Q_T$$

$$\frac{\partial P_E}{\partial t} + (\mathbf{v} \cdot \nabla) P_E + \gamma P_E \nabla \cdot \mathbf{u} + (\gamma - 1) \left[\frac{P_E - P_S}{\tau_{SE}} + \nabla \cdot \mathbf{q}_H \right] = (1 - f_p) Q_T$$

turbulence

$$\frac{\partial Z^2}{\partial t} + (\mathbf{v} \cdot \nabla) Z^2 + \frac{(1 - \sigma_D) Z^2}{2} \nabla \cdot \mathbf{u} + \frac{2}{\rho} \boldsymbol{\mathcal{R}} : \nabla \mathbf{u} + 2\varepsilon_m \cdot (\nabla \times \mathbf{u}) - (\mathbf{V}_A \cdot \nabla)(Z^2 \sigma_c) + Z^2 \sigma_c \nabla \cdot \mathbf{V}_A = -\frac{\alpha f^+(\sigma_c) Z^3}{\lambda}$$

$$\frac{\partial (Z^2 \sigma_c)}{\partial t} + (\mathbf{v} \cdot \nabla)(Z^2 \sigma_c) + \frac{Z^2 \sigma_c}{2} \nabla \cdot \mathbf{u} + \frac{2}{\rho} \boldsymbol{\mathcal{R}} : \nabla \mathbf{V}_A + 2\varepsilon_m \cdot (\nabla \times \mathbf{u}) - (\mathbf{V}_A \cdot \nabla) Z^2 + (1 - \sigma_D) Z^2 \nabla \cdot \mathbf{V}_A = -\frac{\alpha f^-(\sigma_c) Z^3}{\lambda}$$

$$\frac{\partial \lambda}{\partial t} + (\mathbf{v} \cdot \nabla) \lambda = \beta f^+(\sigma_c) Z$$

- $Z^2 = \langle v'^2 + b'^2 \rangle$ is (twice the incompressible yurbulent energy per unit mass
- $\sigma_c = \dfrac{2\langle \mathbf{v}' \cdot \mathbf{b}' \rangle}{\langle v'^2 + b'^2 \rangle}$ is the normalized cross helicity
- λ is the similarity (correlation) length scale

Turbulence modeling assumptions –

- Incompressible and transverse fluctuations
- Turbulent stresses modeled in terms of large-scale gradients (shear)
- NL terms modeled dimensionally (von Karman similarity)

- Physically and empirically motivated ICs and BCs
- Magnetogram-based or dipolar source magnetic field
- Numerical domain from coronal base to few AU

See Usmanov et al., 2018 for more details

Closures and other terms (extra slide)

- Electron-proton collision frequency:

$$\nu_E = \frac{8(2\pi m_e)^{1/2} e^4 N_E \ln\Lambda}{3 m_p (k_B T_E)^{3/2}} \qquad \ln\Lambda = \ln\left[\frac{3(k_B T_E)^{3/2}}{2\pi^{1/2} e^3 N_E^{1/2}}\right]$$

- Classical (Spitzer) electron heat conduction (below 5 $R_\odot$):

$$\mathbf{q}_\mathrm{S} = -\kappa \hat{\mathbf{B}}(\hat{\mathbf{B}}\cdot\nabla)T_E \qquad \kappa = 8.4\times10^{-7} T_E^{5/2}$$

- Collisionless (Hollweg) heat conduction: $\mathbf{q}_\mathrm{H} = (3/2)\alpha_\mathrm{H} P_E \mathbf{v}$

- Turbulent heating: $Q_T = \dfrac{\alpha f^+(\sigma_c)\rho Z^3}{2\lambda}$

- TSDIA closure for turbulent stresses:

$$\boldsymbol{\varepsilon}_m = \bar{\alpha}\mathbf{B} - \bar{\beta}\nabla\times\mathbf{V}_A + \bar{\gamma}\nabla\times\mathbf{v}$$

$$\nu_M = (7/5)\bar{\gamma}$$

$$\nu_K = (7/5)\bar{\beta}$$

Usmanov et al., 2018

$$\frac{1}{\rho}\boldsymbol{\mathcal{R}} = \frac{2}{3}K_R\mathbf{I} - \nu_K\boldsymbol{\mathcal{S}} + \nu_M\boldsymbol{\mathcal{M}}$$

$$K_R = \sigma_D Z^2/2$$

$$\boldsymbol{\mathcal{S}} = \nabla\mathbf{u} + \nabla\mathbf{u}^T - \frac{2}{3}(\nabla\cdot\mathbf{u})\mathbf{I}$$

$$\boldsymbol{\mathcal{M}} = \nabla\mathbf{V}_A + \nabla\mathbf{V}_A^T - \frac{2}{3}(\nabla\cdot\mathbf{V}_A)\mathbf{I}$$

$$\nu_K \approx 0.27 Z\lambda \qquad \nu_M \approx 0.22\sigma_c Z\lambda$$

Modeling NL terms

$$\frac{\partial \mathbf{z}_\pm}{\partial t} = -\mathbf{z}_\mp\cdot\nabla\mathbf{z}_\pm$$

$$\frac{\partial}{\partial t}\langle z_+^2\rangle = -2\langle \mathbf{z}_+\cdot(\mathbf{z}_-\cdot\nabla\mathbf{z}_+)\rangle \sim -\langle z_+^2\rangle\frac{\langle z_-^2\rangle^{-1/2}}{\lambda_+},$$

$$\frac{\partial Z^2}{\partial t} \sim -\frac{Z^3}{\lambda}$$

Boundary/Initial conditions and parameters (extra slide)

Symbol	Description	Value
N_0	proton number density in the initial state at 1 $R_\odot$	$8 \times 10^7\,\mathrm{cm}^{-3}$
T_0	electron and proton temperature in the initial state at 1 $R_\odot$	$1.8 \times 10^6\,\mathrm{K}$
B_0	magnetic field strength of dipole at 1 $R_\odot$	12 G
δv_0	driving amplitude of fluctuations in the initial state at 1 $R_\odot$	$35\,\mathrm{km\,s}^{-1}$
σ_{c0}	normalized cross helicity in the initial state	0.8
λ_0	correlation scale of turbulence in the initial state at at 1 $R_\odot$	0.015 $R_\odot$

Symbol	Description	Value
σ_D	normalized energy difference (residual energy)	$-1/3$
γ	adiabatic index	5/3
α_{H}	constant in Hollweg's collisionless heat flux	1.05
α, β	Kármán–Taylor constants	2, 0.128
f_p	fraction of turbulent heating for protons	0.6
r_{H}	collisional/collisionless electron heat flux transition region	5 $R_\odot$

Usmanov et al., 2018

Spatial Scales Resolved in Simulations

- Resolution $\sim 700 \times 120 \times 240$ in r, θ, ϕ ($r = 1\ R_\odot$ - 5 AU)
- Grid scale Δ is generally within a factor of few correlation scales